Edited by
Aleksander SŁADKOWSKI

FINITE ELEMENT METHOD FOR TRANSPORT APPLICATIONS

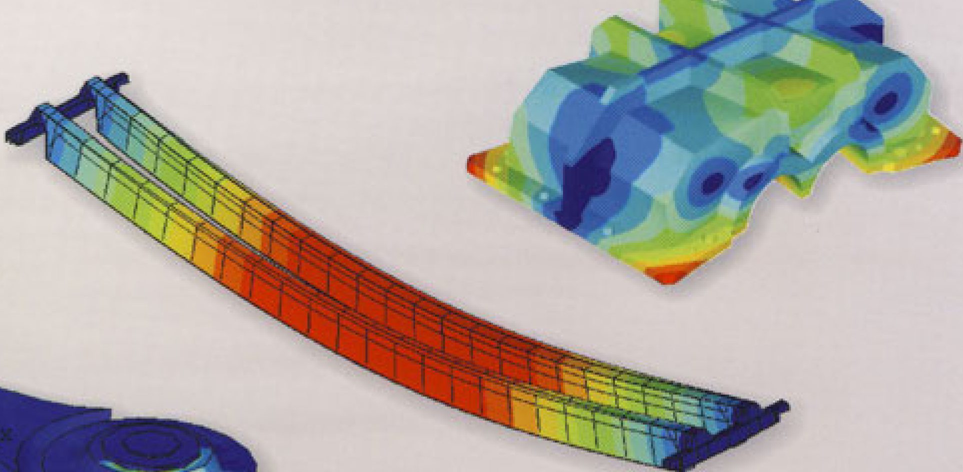

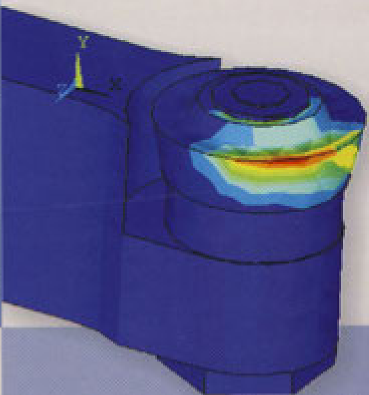

MONOGRAPH

WYDAWNICTWO POLITECHNIKI ŚLĄSKIEJ

GLIWICE 2011

Edited by

Aleksander SŁADKOWSKI

FINITE ELEMENT METHOD FOR TRANSPORT APPLICATIONS

SILESIAN UNIVERSITY OF TECHNOLOGY
GLIWICE 2011

Sergej KROTOV[1], Aleksander SŁADKOWSKI[2]

STRENGTH AND RELIABILITY OF RAILWAY WHEELSET PRESS ASSEMBLY

1. IMPROVEMENT WAYS OF RAILWAY WHEELS AND AXLES ASSEMBLY FOR INCREASE OF LOAD BEARING CAPACITY

Traffic safety, trouble-free operation and life-time of wheel pair of rolling stock and railroad freight cars depends notably on the quality of axle and wheel`s assembly, its durability and load capability. Loaded pressure coupling and interference are widely used in railway transport.

A great quantity of domestic and foreign research investigations are directed to the studies of these assemblies, showing the various ways of assembly load capability increasing [1-6].

However so far the multi-axially and loading variable character and interaction of elements assembly make it impossible to design and forecast the qualitative and force values of connections element interaction, which assures reliability of its functioning. Interaction complexity confirmed by instable assembly process of wheel pair wherein the percentage of defective can come up to 25-30% [7] in conformity of manufacturers information.

Even in the case of assembly quality guarantee confirmed by nice, regular diagram according to technical specifications, when using the wheel pair there are hub's displacement or loosening and fatigue cracks of wheel seat.

First research of railway axles was performed by A. Wohler in 1850. After full-sized axes simulation tests had been made got fatigue curve used for materials fatigue resistance evaluation. He also traced the fundamental association between geometry (coupling and passage form) and fatigue strength [8].

Fatigue cracks progressing in wheel and axle connection and wheel seats are wide-spread defects, depending on connection quality, describable by material properties, joint surfaces preparation method, coupling geometry, interference value, contact pressure and fretting-corrosion value and distribution, in addition to load character [19].

Hub lost is a dangerous defect - defect 71 according to [9]. Displacement of wheel hub is the most dangerous defect - defect 70 [10]. Performed on various stages of transport technical development at increasing of cars carrying capacity and axle load [3] analysis of wheel pairs (rejected as defective because of displacement) has shown, that this type of defect, inheriting to all wheel pair types, is less extended, but catastrophically more dangerous, destructive and detrimental on economic consequences. In [1] is shown that uncoupling of freight cars due to hub lost make up 0,68%, and from the total number of cars, uncoupled due to wheel pair faults, such uncoupling made up already 1,15%! Rejection as defective of wheel pairs 71 [9] presents in actual operating conditions, and like in former times is not always confirmed by control shearing tests.

[1] Rostov State Transport University, Russian Federation
[2] Silesian University of Technology, Poland

Analysis of wheel misalignment [1] has shown that wheels are displaced from axles in an outward direction when passing the switches and inwards direction when passing curved tracks.

In [10] is noted that when testing a big amount of wheel pairs, assembled by application of heating method with elastomer GEN-150, cases of wheel hub displacement and crank as a result of incomplete polymerization of coupling covering were detected.

At the present time the basic method of wheel pair formation is the pressing of wheels on axle with hydraulic presses. Such connection should assure transmission of torsional moment and forces by wheel pair without slacking and wheel displacement from axle [11]. The problems of wheel pair assembly with sub-zero treatment is studied fundamentally [12]. Various surfaces with polymer abrasive galvanic materials were used in machinery and transport.

Surface nitriding, oxidation are shown as means of increasing bearing ability at various seat types [1, 13] mounting by gluing and pressing are widely used abroad; their positive effect is obtained at electric rolling stocks operation.

2. ASSEMBLY EFFICIENCY WITH GUARANTEED INTERFERENCE UNDER STATIC AND DYNAMIC LOADING

Qualitative evaluation proceeding of assembly is possible in terms of least shearing force or torsional moment, which will not lead to axial or circular displacement of conjugated elements. Conventionality of such assessment is obvious. At the present time the main indicator of assembly efficiency when its construction is considered the value of end compressing force with good compressing force diagram [11]. In practice, the relative durability of shearing force to diagram pressing force is determined post-factum. By increasing of pressing force, as a rule, shearing forces are increasing too, but there are no clear linear dependence, as technological and geometric parameters have a large influence [1, 2, 11, 13, 14].

Analysis of works on static strength of car's wheel-axle assembly allows conclusion that final pressing force value depend on tightness, hub's length, quality of conjugated parts, mechanical properties of axle and wheel material, applied lubricant, pressing speed, temperature conditions of conjugated parts and a lot of other factors. The main factor is an interference, associated with diameter; in the modern context interference range is 0,18 – 0,24 mm. Interference value (excl. external loading factors) actually determines the value of contact pressure and assembly parts, which pressure values should not exceed proportionality limits for axle and wheel.

In view of ambiguity of parameters, determining assembly efficiency, the final pressing force cannot be a measure for durability assessment; it is confirmed by comparative inconsistency of operational displacements. It must be also admitted that possibilities of increase of wheel-axle assembly static strength when axle rolling are limited, it must be considered when further increasing of axle load. For RF railways rolling stock when actual loading wheel is 195 kN pressing 785 kN for each 100 mm of diameter is recognized. According to loading analysis it is known that side forces applied to wheel flange don’t exceed 98-118 kN, when axle loading is 230,5 kN, and can’t be more than 150% of wheel-to-rail load by derail criterion. Therefore, acting axial forces can’t be more than 25% of minimal pressing force and by possible shifts its relative value should be 0,25 and less. As a reason of such a sufficient reducing of bearing ability of wheel to axle coupling under operation scientist and specialists considers the availability and effects of reversed bending on wheel-axle assembly.

Operating practice shows that durability of assembly with guaranteed interference on axial shifting and cranking change with time under dynamical forces. At the same time it is discovered when repairing that assembly strength is much higher than a determined one. Factors influenced long-time strength when operating are known.

Attraction of mating elements which leads to galling of mating surfaces and thereby reduce interference on sliding areas and bearing ability of assembly [1, 3].

Fretting-corrosion, caused by attraction of mating elements when cyclic loading, is attended by fretting, electro-erosion destruction, which from one side is conductive to development of contact-fatigue effects and splitting in axles [13], and from other side – not removed confrication products can bring to increase of assembly strength [1, 5].

During contact relaxation the whole durability of assembly is reduced. Relief of residual compressive stress got when mechanical surface preparation, can increase assembly durability [1, 5, 12, 13]. Contact confrication corrosion occurs when attraction (sliding) of surfaces is available, and in wheel-axle assembly with dynamic load and repeated deformation it is always the case. Attraction availability is determined in some researches [3, 5, 12, 13]. In [3] it is shown that when stress increasing the area of static contact is reducing, when vertical load per axle of 49 kN it makes up 65,6%, when 147 kN – 27%, and when 196 kN – 16,2%. Reducing of contact area in [3] is confirmed by operating data when speeding-up. The authors [6] note that there are no registered cases of wheel displacement from axles under empty cars.

Reasons of wheel-axle assembly shear strength reduction are observed in works [5, 8]. It is noted that static bending load doesn't cause shear strength reduction, while rotational bending reduces bearing ability of assembly. These facts were confirmed by benchmark tests. Accordingly [5] one of the reasons of bearing ability reduction is sliding of metal surface coating caused by rotational bending. The authors [5] notice that self-pressing-out of wheel-axle assembly without axial force application is possible. In their opinion it is caused by expulsive force, which occurs due to elongation-compression difference of axle fiber and wheel hub. Possibility of occurrence of such strength was confirmed by cantilevered rotational bending [5]. Rise in loading frequency can cause more assembly strength reduction due to speeding-up of element's slipping, what is associated with friction coefficient reduction. At the same time, as the authors notice, sliding is not the only reason of assembly bearing ability reduction [5], because ultimate bearing ability depends on coefficient of sliding friction value, which is changing over wide range, and in this case is nonzero, depends on seating conditions and motion state [4, 5, 14].

In [13] is stated that reciprocal displacements of wheel and axle assembly points during the addition with deformations of the same sign (direction) cause slipping and as result reduction of total wheel-axle assembly strength.

Thus, this review shows that main reasons of bearing ability reduction of assembly with guaranteed interference under influence of reversed bending are deformations of connection elements and their relative slipping and as a result their ability to move without additional external load.

3. REVIEW OF THEORETICAL SOLUTIONS ON STRENGTH AND BEARING ABILITY OF WHEEL-AXLE ASSEMBLY

Traditional theoretical computation of static wheel pair durability include three main stages: determination of operating forces and selection of analytical model, loads estimation and strength assessment.

In practice the recommended computations of wheel and axle durability [15] and wheel-axle assembly are computed separately. Therefore these methods are conventional as they don't take into account dynamics of loading, deformation, mechanical impact and interaction of wheel pair elements [16, 17]. Complex methods of elasticity theory [23, 24] or numerical calculations of finite element schemes [18-22] should be applied for more exact calculation of wheels and axles, for example, for loading calculation caused by heat current influence when braking.

In the research of E.S. Savvushkin [18] concerned with contact pressure in wheel and axle hub when pressing for simplified cylindrical assembly model, with the assumption that there is no friction forces on the contact surfaces was stated, that contact pressure is divided irregularly on hub length, concentration on hub's ends is 1,75 times larger than pressure value according to Lame Formula.

In the work of P.V. Shevchenko [17] much attention is given to investigation of crack formation in car axles and developing of meaningful measures for their durability and life-time increase, as well as theoretical justification and creation of contact pressure distribution. While using functions and loads and motions according to A. Lyav for axisymmetric problem, radial, tangential, axial and shearing stresses in wheel seat were determined. The problem of contact pressure distribution between hub and axle was solved according to recommendations of A.A. Popov by approximate method of point-like contact. On this basis the author recommends formulas for estimation of axial force, shearing force and torsional moment limit values, which are theoretically important, as actual contact pressure value is always individual and unknown. Experimental original data of assembly durability research at dynamic (unbalanced) load are of interest, they confirmed that relative dynamic strength Ψ=75-80% is lower than a static one Ψ=200-220%. So, in the author's opinion to break wheel-axle assembly when it is working less force than pressing force is needed. This fact confirms the above given idea that the value of final pressing force does not determine durability and reliability rate of wheel-axle assembly. The idea is also expressed about refinement of analytical models, which take into account of external loads and motions, and it essentially corresponds with design model of wheel-axle assembly, represented by us [23].

V.I. Sakalo [20, 21] in his works propose the estimation methods of stress and strain state calculation with application of finite element method (FEM) for applied contact problems for railway rolling stock. Particularly to solution of the problem of wheel-rail contact, seating surfaces contact like wheel-axle assembly it is recommended to apply universal scheme of strain relaxation method. It is a physical interpretation of the process of finite element cross-points moving determination, simple and shearing stresses, slipping and assembly units coupling, when iterative process convergence acceleration for models with a large number of equations.

In addition to illustrations of seating connection calculation according to above mentioned method in [20, 21] is showed that tabular analytical models for wheel pairs and wheel-axle assemblies can be applied adequately for practical purposes. Further it gave occasion to selection of wheel pair design model to determine straining and internal force factor, as well as wheel-axle assembly model to determine adhesion and sliding zones.

In the work [22] calculation are developed and performed on determination of contact pressures and loads in wheel seat of the axle for wheel-to-hollow-axle connection, compared to standard solid one, through finite element method. Calculation results while tightness value is 0,1 mm shown that contact pressures are distributed irregularly when pressing, with sharp rise along hub edge. As the authors notice, it serves to occurring of edged fretting-corrosion on surface while in operation, which reduces axle fatigue strength. It is also noted that loadings don't exceed flow limits. In [22] estimation of loadings in axles is conducted on amended design model with application of external loads, exerting on wheel pair of 4-axle low-sided car on trucks of bogie by CSRI – H3O by speed of 120 km/h. Mode of load distribution in wheel seat and before-wheel seat and before neck beginning. Distribution in whole and solid axle is almost the same. Estimation procedure, explained in [22] allows wheel pair elements estimating on PC, assessing their stressed state, but amendment of design model by force factors, serving to is required.

Applied new calculation methods of stress and strain state of wheel-axle assembly build a complete picture of stress values, not taking into account elements relative motions without considering reciprocal displacements of components. In mechanical engineering special attention is given to the operations and design of pressing and thermal assemblies. It is associated with distinction of loading and operational conditions of most class of assemblies. Distinction of loading conditions create specific prerequisites for selection of design models of heavily-stressed elements, among which are wheel-axle assembly of car and rolling stock wheel pair.

Sources review, analysis of wheel pair loading and necessity of wheel-axle interaction evaluation allow summarizing research objectives:

- development of press assembly finite elements model to determine dependence between assembly force and geometrical parameters;
- development of wheel pair finite elements model which allows numerical experiment calculating of deflected mode of wheel, axle, and press assembly to determine wheel-axle assembly bearing ability parameters;
- performing of multivariate statistical analysis of wheel pair deflected mode research results including discriminatory analysis to classify actual state and forecasting of wheel-axle press assembly with mathematical models, which allow using analysis results in monitoring system wheel pair and its press assembly.

Before we present some results of our researches, let us emphasis some simulation system problems based on FEM, solution methods and technologies used not only by transport scientists to study deflected mode of various objects.

4. APPLICATION OF FEM FOR DEFLECTED MODE DESIGNING

The practical aspect of conducted researches with application of numerical method is undoubtedly aimed at improvement of work of some units of mechanical-engineering and building constructions, rolling stock etc., understanding of damage occurrence regularity, forecasting and prevention of dangerous situations enabling higher safety of exploitation of objects under investigation and their safe operation.

In fact all scientific developments studied by us can be presented as the following algorithm which comprises main operations of numerical simulation based on finite elements method.

Reasons for choosing the method of elastic theory problem solution in case of interference mounting on the basis of finite elements method. It is necessary to choose crucial ratio, for instance, based on possible displacements principle.

Then calculation methods algorithm is described; the algorithm includes fundamental concept of finite elements method, domain finite elements modeling (domain discretization), function finite elements modeling, stiffness matrix and local coordinate system load vector determination, global stiffness matrix and global load vector formation [25-26]. Thereafter the system of finite elements algebraic equations should be solved, deformations and loads, displacements should be determined [27].

The following methods are used: accounting methods of linear restriction in symmetric system of linear algebraic equations, such as Lagrange multiplier method [28], penalty function method [29], global stiffness matrix and displacement vector reducing method, Webb's method [30] and others. Then finite elements modeling of wheel-axle assemblies with the most acceptable method is performed. Structure of finite elements restraint matrixes corresponding to wheel-axle assemblies is taken into account [31]. Special features of software implementation are illustrated [32-33]. Modified finite elements are applied if needed. Particularly, asymmetric finite elements schemes are often applied for railway transport wheel pairs. It also concerns wrought and banding wheels, as well as a lot of solids of rotation which can be estimated by FEM. Then everything depends on the problem set for the researchers. So, in the work [34] the following major questions are considered in addition to the mentioned above: hub-to-axle fitting; pressing of several round washers into plate, restricted by Pascal snail; pressing of round washer to plate with non-constant interference; washer-to-round-plate pressing, the washer being loosen by eccentric elliptical manhole. Finite elements modeling of rotor end-winding retaining ring and thrust washer wheel-axle assembly with complete water cooling is completed upon problem setting, 3D FE model of turbo-alternator retaining ring assembly is used; validity of obtained results is estimated. Axisymmetric retaining ring assembly FE models and simulation system ANSYS [35] were used. So the questions observed with numerical calculation methods are quite various.

The main results include investigations of three-dimensional stressed and strained state of pressure coupled turbo-alternator retaining ring and thrust washer with complete water cooling in quiescent mode and typical alternator operation and further appropriate recommendations.

One of the first works devoted to investigations by means of load finite elements method in case of collar on axle of infinite length pressing is the work of B. Parsons and E.A. Wilson [36]. The authors used FEM to determine stiffening behavior of the collar by calculating influence coefficient in units placed on the internal surface of collar finite element model. They used classical elasticity theory method based on A.I. Lurye's works to determine axle stiffness [37].

Solution of problem of collar to axle of finite length pressing is given in the work [38] which is development of the method worked out in [37]. The described method allows taking into account crimping of surface microroughnesses by injection of simulated contact layer which suppleness is taken from the work [37]. Application of the given methods is restricted by axisymmetric components research.

To solve pressing problems a general analytical method based on plane elasticity methods developed by G.V. Kolosov and N.I. Muskhelishvili was offered by D.I. Sherman [87], and D.I. Sherman [39], N.D. Tarabasov [40] and others got a range of problem solutions. These works are devoted to stress state analysis of components without axial symmetry occupying simply connected domain, the circle being reflected by means of polynomial function [80]. Such approach for pressing problems solution is only applicable to domains for which the analytical function exists. For real design elements it is not always possible to choose such a function and even in the cases when it can be done [41], researches with methods based on application of complex mathematical tool are complicated and tedious, it reduces the practical value of the method not lowering importance of this method for theoretical investigations. That is why when performing engineer works requiring design multiparameter and multiversion analysis on the stage of constructions, it is more reasonable to apply numerical techniques.

In [42] main finite elements method algorithms and techniques applied to wheel-axle assemblies are explained circumstantially and thoroughly. The aim of this research was the ability to forecast fatigue occurrence of wheel pair wheel-axle assembly. Many authors use parameter $F_1 = \tau\delta$ called wear parameter, where τ is shearing stress and δ is relative shear. Parameter F_1 is presented as friction work per area unit. Then one more parameter is added $F_2 = \tau\sigma\delta$ called fretting parameter, i.e. wear parameter is added by stress σ which exerts parallel to contacting surface.

Many authors have pointed to these parameters Waterhouse [43], Fellows et al. [44]. In this work, basing on Vingsbo and Soederberg [45] they differentiate three various fretting forms: a) form with very limited surface damage without fatigue crack; b) mixed form of axis slipping, with slight wear and oxidation damage, reduced life-time due to fretting influence; c) slipping with serious wear-blemish added by oxidation, with localized crack.

Further in [42] different simulation techniques of surface condition in wheel-axle assembly, regard to elastic and elasto-plastic contact, slipping zones simulation with FE. It is stated that if relative side shears between hub and axle are not too big, the assumption of linear friction law is accepted. But when obtained results are not confirmed by lab tests, process simulation with regard to nonlinear friction law is recommended.

In conclusion inferences were drawn about complexity of studied phenomenon; many qualitative and quantitative parameters are quite sensitive to finite elements value. Relative models illustrated in literature can be divided into simple classic criteria, which give approximate result; techniques simulating fretting-fatigue without cracks, and “fracture mechanics” techniques simulating occurrence of fatigue cracks. In the work [93] the author offers the so called multiaxial symmetry condition and appropriate “amplification factors” should be added to achieve required accuracy when determining stresses state in wheel-axle assembly.

Therefore on the basis of short review of some literary sources we can conclude that problems and tasks solved by numerical calculation methods based on finite elements method are quite numerous and various.

To optimize wheel pair design in the work [46] the following key questions were raised:

- comparison of software used by wheel pair design;
- development of wheel pair design methodology;
- increase of wheel pair life-time;
- railway transport safety growth;
- cost saving at wheel pair production and service.

4.1. The choice of calculation method and FEA software

To study the pressing joints, namely, to this class of problems concerns the wheel - axle connection, can be used a variety of software based on FEM. The difference relates primarily to the chosen formulation of the problem. If you can’t take into account possible non-axisymmetric problem, the problem is greatly simplified. On the other hand the choice of software is greater. The problem of the generation of FE meshes solved more easily. In this case it is easier to coordinate meshes of interacting bodies, but also have the opportunity to use a mesh with many nodes.

As example, for calculation of such fields of stresses different FEA packages may be used, but usually thus it is necessary to use nonlinear algorithm and special contact elements. The authors developed algorithm [61], which has allowed using possibilities of NASTRAN package in linear setting. This task analytical solving is not obviously possible, however FEM application allows finding its solution. In particular, for its execution we used the application package MSC/NASTRAN for Windows. The examined process of wheel pair forming can be realized in program with GAP – elements usage. Thus the task will be solved with usage of algorithms of nonlinear static in three-dimensional setting. We can, certainly, with the help of two radial sections cut any layer and consider contact interaction of axis and wheel for layer elements. However it considerably complicates setting, for which sequentially it is necessary to solve a set of contact interaction in wheel-axis pair tasks for their different relative positions during press fitting. The new technique, founded on the axisymmetric calculated scheme application was developed.

We shall consider all over again the task about stresses allocation and, in particular, contact stresses in formed wheel pairs. For this purpose we solve with the help of NASTRAN the axisymmetric task about common deformation of wheel and axis at preset tightness. For the first we assume that the friction coefficient between contacted surfaces of the wheel and axis is infinite. It means that in such a way it is possible to model a complete adhesion that takes place after durable maintenance of wheel pair.

During FE-model creation we used three-nodal axisymmetric finite elements which total quantity is equal to1548. Thus there were two finite - element grids created, one for wheel, and another one for an axis. Total quantity of nodes is 962, including 17 contact pairs. At FE - mesh choice for wheels the guidelines of paper [62], stipulated by necessity of solution exactitude security, were used. In calculation real properties of wheel steel were included. With regard to constructive reasons for creation of tightness during wheel fitting its diameter of a hole in hub was executed on 0,25 mm less, than a diameter of hub part of axis. In appropriate pair nodes on a contact surface “wheel - axis” it was necessary to set boundary conditions, aspect of which is described in paper [61].

Defined deficiency of NASTRAN or FEMAP preprocessor is the fact, that it does not allow to set boundary conditions such as Constraint Equation if Δ=const. We managed to overcome this deficiency with regard to the necessary to set also the boundary conditions, which bounds the wheel, as the rigid whole, displacement in axis Z direction.

On fig. 1 [63] not-deformed FE-mesh of an axis and a wheel (fig. 1a), as well as the contact zone in an expanded scale (fig. 1b) is represented. At FE-grids choice the basic principles of paper [62] were used. While using them it was possible to minimize the calculations error, which was stipulated by grid choice, and at its minimum possible amount of nodes (with limitation from the point of view of an error) to provide solution of peak efficiency.

However, as the principal attention in paper is given to contact interaction of the wheel and the axis during wheel pairs forming, it was possible to reduce the elements number on width of the wheel disk. It is still possible to mark, that a series of wheel pair’s constructions have special gnowing-through for wheel pair’s pressing-out FE modeling of this gnowing-through is well seen on the enlarged fig. 1b.

In fig. 2 distribution of radial stresses in a sprocket having a construction on Polish standard PN-92/K-91019 920/200s, at its pressing on an axis represented, to appropriate construction PN-92/K-91048 B 200s is presented. Three positions of a sprocket concerning an axis in pressing process are reduced. As calculations display, the level of stresses in original and intermediate positions is much higher, than for formed wheel pair. And, for a maximum permissible tightness of the sprocket equal of 0,25 mm, origin of the plastic zones localized in a zone, adjoining to an internal surface of a hole in a nave of a sprocket is possible. Accordingly, similar plastic zones may take place on according parts of an axis.

The process of creation of wheel pairs is enough a crucial technological operation during which change of pressing effort is fixed during creation of wheel pair. The obtained profile is recorded and forms the basis for the rejection of formed wheel pairs. Such profile should match theoretical one which is obtained by design way.

Besides, numerical experiments during wheel pressing on axle were performed; the experiments allowed to determined contact vertex percentage spread in wheel pair elements assembly with 0,18 mm interference. It turned out that irrespective of wheel shape 80% of displacements fall on wheel and 20% on axle; thus it is possible to make conclusion about stress spread in contact. On fig. 3 comparative analytical diagrams and diagrams got by numerical experiment of wheel pressing on axle are shown. It is necessary to mark, that the construction of a considered wheel provides execution of a special hole and groove for pressing-out wheel pair. On the introduced profile in an average part there is the local wave, shown as an arrow. This wave will match the moment of the beginning of interaction of a wheel and an axis in a zone of the indicated groove.

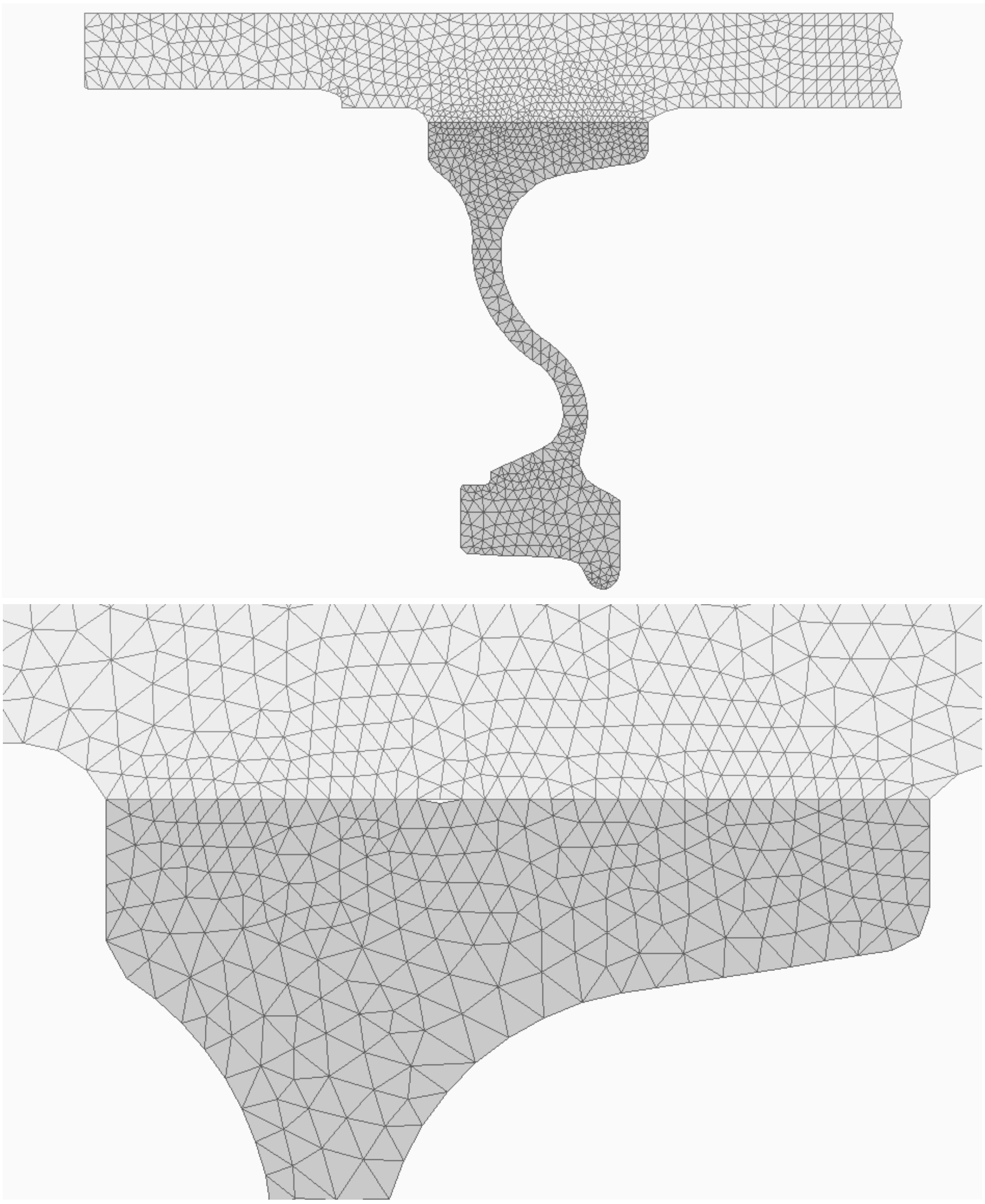

a

b

Fig. 1. FE – discretization of the pair wheel – axis (axisymmetric model)
Rys. 1. Dyskretyzacja MES pary koło – oś (osiowosymetryczny model)

Nowadays there is a great amount of different constructions of solid-rolled vehicle wheels, which are intended for different types of carriage rolling stock. Accordingly, besides the trial function, they execute a series of additional ones, for example, initial damping or lowering of noise. Within the framework of this paper we shall not consider those or other advantages of such wheels. We shall accept, as due already existing constructions. The greatest problem is the requirement to lay down all wheels in identical conditions of wheel pairs forming for analyzing influence of their constructions on their deflected mode. This problem is stipulated by the fact that each wheel is assumed to use its own axis. Thus the wheel hub may be both more widely, and already hub part of an axis. Diameters of holes in hub for different wheels differ among themselves. And, at last, the difference in technology requirements for tightness has a great meaning.

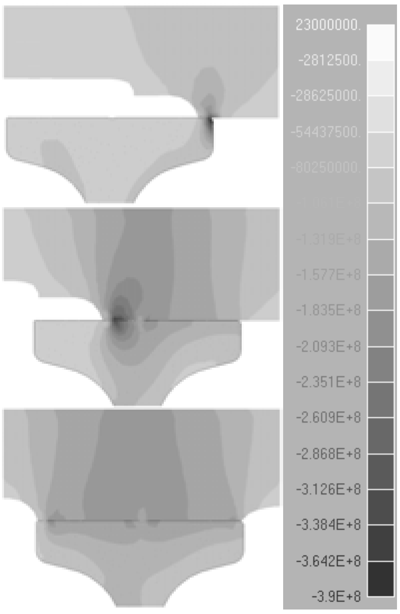

Fig. 2. Distribution of radial stresses in a wheel and axle during creation of wheel pair
Rys. 2. Rozkład naprężeń promieniowych koła i osi podczas tworzenia zestawu

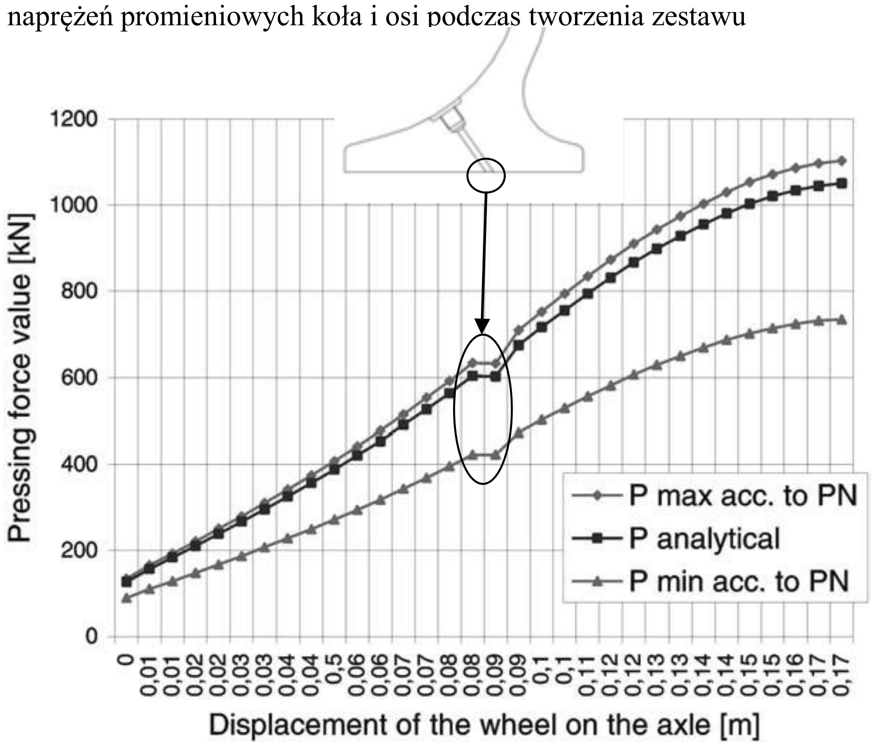

Fig. 3. Theoretical diagram of pressing the wheel onto the axle: wheelset PN 920/200s
Rys. 3. Teoretyczny wykres dla siły wcisku koła na oś: zestaw wg PN 920/200s

For unifying such press connections the analysis of different wheel pair's constructions, which are used on railways of different countries of the world and, first of all, on the European railways, was carried out. From all diversity of wheel constructions the most typical were selected and they are shown on fig. 4. For analysis of wheel construction influence on their deflected mode, stipulated by wheel pairs forming, there were selected wheels having a diameter of a hole in hub of 185 mm. As the general axis we used the axis with construction, appropriate to Polish standard PN-92/K-91048 of A type. The analysis was done for two tightness values of 0,18 and 0,25 mm, minimum and maximum, accordingly.

The main tendency of modern machine industry is the usage of wheels as an initial elastic unit of a coach, the vertical rigidity decreasing of that promotes lowering of dynamic loads, which are transmitted on sprung masses of a carriage rolling stock. For this purpose on wheel disks there were executed corrugations of different construction in the central part of the disk. The rim location of the wheel concerning a hub may be symmetrical, as for the wheel fulfilled according to Polish standard PN-92/K-91019 920/185s (fig. 4a), or nonsymmetrical 920/185a (fig. 4b). Central corrugations and, accordingly, a vertical rigidity of the wheel may be larger and smaller, comparing, for example, the wheel of Huta "Gliwice" S.A. production - drawing TT-2537 (fig. 4c). Enough obsolete construction is the wheels with direct slant disks (conic), for example, the same production - drawing TT-2990/KO (fig. 4d). The wheels of GOST 9036-88 standard, which are used on railways of the former USSR, are similar to above mentioned. The wheels with S-figurative disk of Bonatrans A.S. Bohumin production - drawing 455.0.212.000.12 have more perspective construction (fig. 4e). And, at last, the last wheel of Stablimento di Lovere Lucchini production (fig. 4f) has enough original construction with C-figurative disk. The main results of calculations are also shown in the tab. 1, where for the mentioned above tightness values the maximum equivalent stresses are defined according to energy criterion of Von Mises.

Table 1

Maximum stresses levels in wheels of different constructions for extreme values of tightness

Wheels fig. 4 no.	The tight-ness (mm)	Radial stresses σ_r in the wheel disk		Maximum equivalent stresses in the wheel according to Von Mises criterion
		min (MPa)	max (MPa)	
A	0,18	-63,4	18,4	193,7
	0,25	-88,0	25,9	268,8
B	0,18	-56,9	17,5	214,9
	0,25	-79,0	24,2	299,5
C	0,18	-78,8	29,0	190,8
	0,25	-109,4	40,3	265,6
D	0,18	-62,7	12,0	189,1
	0,25	-87,0	16,6	258,5
E	0,18	-45,1	12,6	201,7
	0,25	-62,6	17,5	280,1
F	0,18	-80,5	16,9	192,1
	0,25	-111,8	23,4	266,9

These stresses for all wheels are achieved on an internal surface of the hole in hub. On fig. 4 these places are shown as $\otimes$. Difference of different wheels in this case is only that of transition zone hub-disk symmetric location, these places are also symmetric to axis of hub, transiting through the middle of the hub. At disk displacement, the appropriate zone of maximum stresses displaces on an external part of hub in direction of the disk displacement.

Magnitude of such stresses in wheel built-up position does not exceed a yield stress of wheel steel; however, during wheel pair forming it is possible plastic deformations zones creation in zones adjoining to the hole in hub. The latter proves that fact, that if we compare maximum stresses (21,6 MPa) during wheel pairs forming with construction tightness of 0,18 mm fig. 4e and a range of radial stresses for the same wheel in the formed state ($-45{,}1 \le \sigma_r \le 12{,}6$ MPa), we can see, that stresses during forming may be almost two times larger, than for formed wheel pair. Places of localization of the greatest and the least radial stresses in wheel disks, which values are shown in the table, on fig. 4 are marked by signs $\oplus$ and $\ominus$, accordingly.

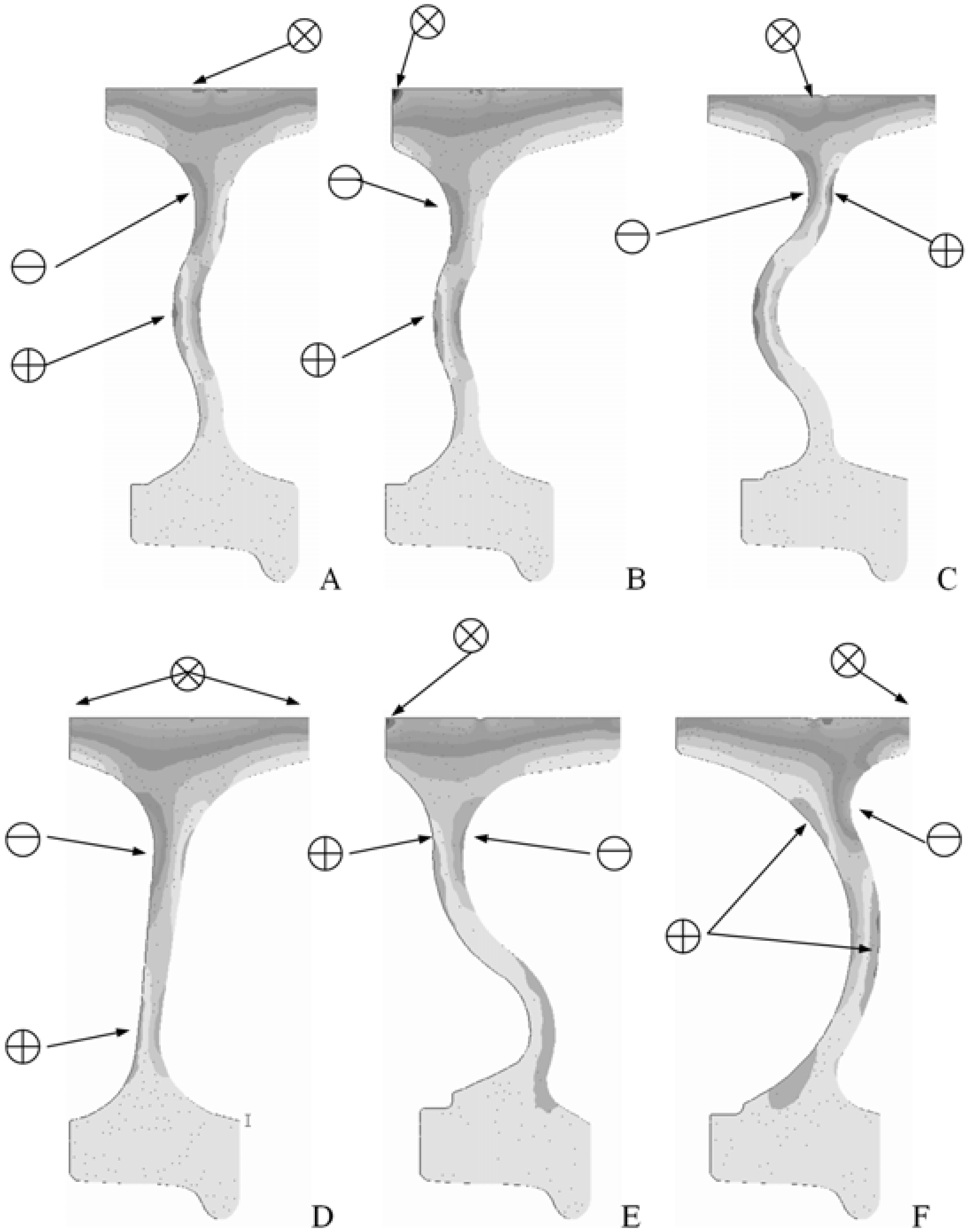

Fig. 4. Radial stress in vehicle wheel of different constructions after wheel pairs forming (descriptions of constructions are in the text)

Rys. 4. Naprężenia promieniowe w kołach różnych konstrukcji po montażu zestawów (opisy konstrukcji są w tekście)

Calculations for ten types of European wheels with 0,21 mm interference are provided to determine disk form influence on stressed state due to wheel pressing on axle (examples of such solutions for 3D models are shown in fig. 5).

The analysis has not proven any significant influence of the wheel geometry on the stress value (mesh geometry and the wear of wheel rolling surface). The impact of hub symmetry (or asymmetry) is great. In the case of the asymmetrical hub, the stresses accumulate in this part of the hub, where the wheel mesh is located, and they diminish in the opposite direction. The uniform distribution of stresses in the wheel and axle characterizes the wheel with the symmetrical hub. Stresses arising in rising the wheel hub material during the pressing process on the set axis take a value of 200 MPa. The plasticity boundary of R7 steel is 360 MPa. Therefore, the pressing process causes the formation of stresses, whose value is from 30 to 50 per cent of plasticity boundary. Therefore, high stresses have a great influence on the durability of railway wheels.

Influence of dynamic load was studied, speed being 100-300 km/h, axle load – 16-32 tons. The values of dynamic load of railway wheelset were accepted according to the UIC recommendations. The loads were defined as the concentrated force, three times larger than the static loads. However, like in the case of static loads, the dynamic loads are also defined as the concentrated forces. The values of these stresses are three times greater than stresses due to carriage weight; the distribution is similar. The wear of the rolling surface of the wheel does not have a great impact on the value and distribution of these stresses.

Then one of the solutions is shown to determine sustained braking influence on deflected mode of various wheel types (fig. 5c). The concentration of stresses in this part of the mesh suggests that the decisive impact in the superposition is borne by dynamic stresses and stresses due to braking.

Influence of mating surface diameter was also investigated.

Results of the work done are the following key conclusions:

- finite elements map impacts on spread of stress fields, temperatures and displacements;
- wheel and hub map geometry impacts on stress fields;
- wear rate analysis has shown that this factor is important when studying stressed state at braking;
- performed analysis shows the importance of finite elements scheme correction for research.

Certainly, only small part of research results is given here.

Thus, any researcher who applies finite elements analysis for wheel pair design can find answers on questions when determining tactics and strategy of wheel pair elements design with various combinations of external load factors, wheel pair geometry, wheel-axle assembly parameters as well as when choosing simulation system as a research tool.

Then we study some calculation results of modern wheel pair of RF railways based on simulation system [49]. When determining accuracy of deflected mode, much emphasis was put on wheel-axle assembly zone because as damage statistics mentioned below shows, defects and damages of wheel-axle assembly rank high in general classification, they are dangerous for people’s health and rolling stock operation safety.

4.2. Impact of loading conditions increase on wagon wheel-axle assembly bearing ability

Considering that wheel pair bearing ability is inextricably associated with wheel-axle assembly reliability rate, when stiffening of wheel pair operating conditions due to load growth and speed increase, increased requirements are imposed on wheel-axle assembly reliability rate. According to the analysis of wheel pair damage statistics on US railways in the observation period 1975-2006, damage from wheel pair defects made up USD 380,5 million, 14,5% - USD 55,4 million fall on wheel-axle assembly defects (broken hub and loose wheel) [47]. Picture of wheel pair damaging over the period of 13 examination years in USA [47] according to special form - TRAIN ACCIDENTS BY CAUSE FROM FORM FRA F 6180,54, where defects data for wagon and locomotive wheel pairs are presented, is shown below. In tab. 2 there are data from all the roads, states and districts.

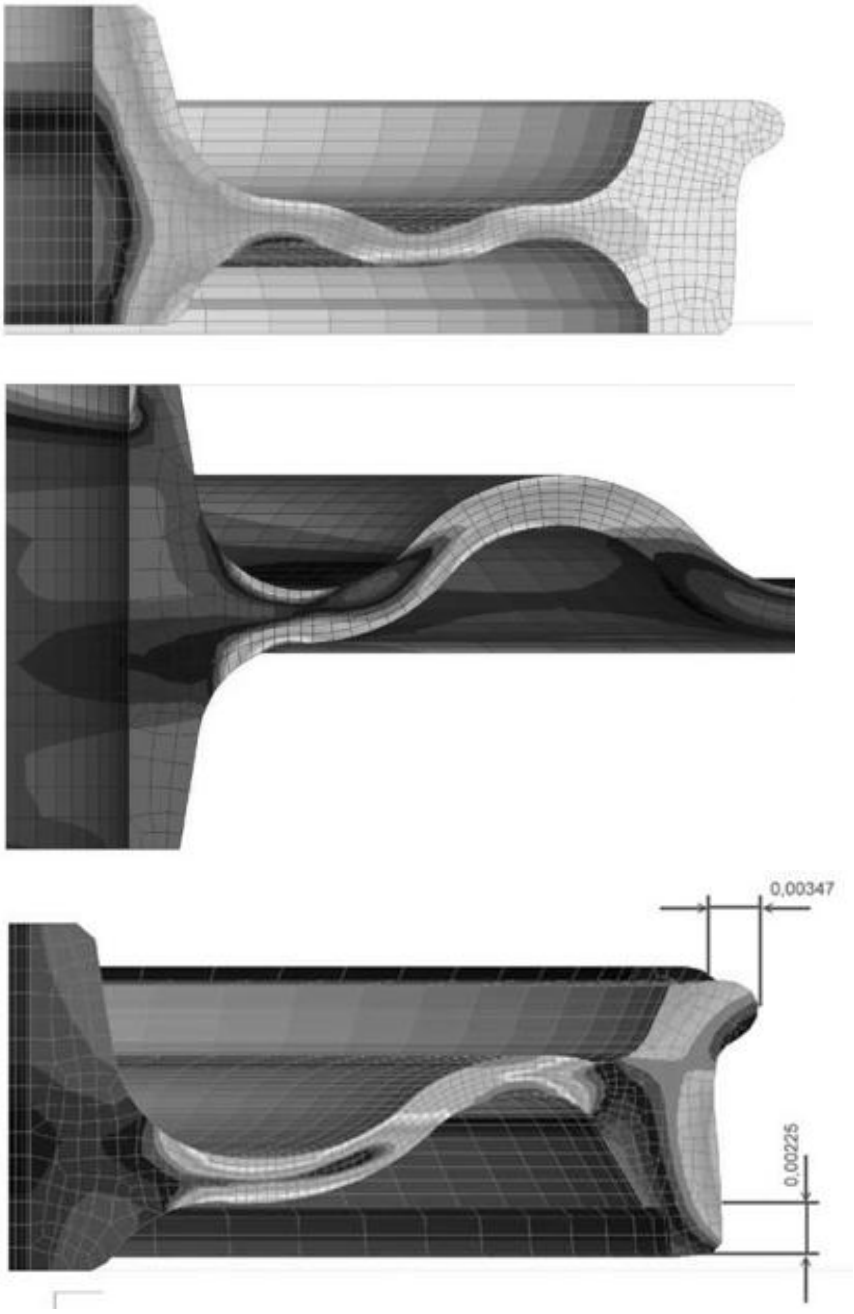

a

b

c

Fig. 5. Distribution of stress (von Mises) for different wheels analyzed by means of displacement method under different kinds of loading: a) wheel – axle pair PN 920/185a for 0,18 mm interference; b) wheel – axle pair ČD, Bohumin, fig. no. FWG\302.0.02.001.007, 0,21 mm interference and carriage weight, axle load 22,5 tons per axle; c) wheel – axle pair ČD, Bohumin, fig. no. 455.0.212.000.12, results of simulation of sustained braking (geometry of maximum displacements in both directions has also been shown)

Rys. 5. Rozkłady naprężeń (wg Misesa) dla różnych kół przeanalizowano za pomocą metody przemieszczeń w ramach różnego rodzaju odciążeń

Table 2

Train accidents caused by damage of wheels

Specific causes:	Total		Type of Accident			Reportable Damage		Casualty	
	Quantity	%	Collision	Derailment	Other	Amount	%	Killed	Nonfatal
Broken flange (WAGON)	354	7,9	3	345	6	40 259 905	10,6	0	18
Broken flange (LOCOMOTIVE)	8	0,2	-	8	-	430 276	0,1	0	13
Broken rim (W)	582	13,1	1	565	16	102 803 055	27,0	0	22
Broken rim (L)	15	0,3	-	14	1	1 088 575	0,3	0	2
Broken plate (W)	530	11,9	-	512	18	73 120 004	19,2	0	47
Broken plate (L)	16	0,4	-	14	2	464 296	0,1	0	1
Broken hub (W)	116	2,6	-	116	-	13 924 275	3,7	0	3
Broken hub (L)	4	0,1	-	4	-	1 689 946	0,4	0	0
Worn Flange (W)	1 460	32,8	18	1 427	15	28 029 167	7,4	0	22
Worn flange (L)	99	2,2	-	99	-	5 820 886	1,5	0	7
Worn tread (W)	67	1,5	1	64	2	6 728 130	1,8	0	1
Worn tread (L)	5	0,1	-	5	-	351 668	0,1	0	0
Damaged flange or tread (flat) (W)	204	4,6	1	200	3	15 679 079	4,1	0	11
Damaged flange or tread (flat) (L)	14	0,3	-	11	3	813 026	0,2	0	1
Damaged flange or tread (build up) (W)	161	3,6	-	159	2	10 380 824	2,7	0	0
Damaged flange/tread(build up) (L)	2	0,0	-	2	-	22 826	0,0	0	0
Loose wheel (W)	328	7,4	3	324	1	39 474 295	10,4	0	44
Loose wheel (L)	8	0,2	-	8	-	526 731	0,1	0	0
Other wheel defects (W)	392	8,8	14	363	15	28 602 483	7,5	18	67
Other wheel defects (L)	43	1,0	-	38	5	3 798 691	1,0	0	2
Thermal crack, flange or tread (W)	46	1,0	-	46	-	6 612 950	1,7	0	1
Thermal crack, flange or tread (L)	2	0,0	-	2	-	304 838	0,1	0	0
Total	4 457	100	41	4 327	89	380 934 187	100,0	18	262

In the beginning of examination axle load of freight cars was 285 kN/axle, further it grew up to 304-343 kN/axle for various car types. It is obviously that further load increase can result in reducing of wheel pair bearing ability, particularly, of wheel-axle assembly. That's why assessment of wheel-axle assembly bearing ability when stiffening of wheel pair operating conditions is of much importance, as the question is in traffic safety.

Since physical simulation of wheel and axle interacting processes is quite difficult, numerical simulation is possible, as it is quite a useful tool for durability and reliability rate assessment of various items that was mentioned above.

All the above mentioned programs «ANSYS», «NASTRAN», «COSMOS» etc. have priority in problems of calculation accuracy and speed. Primary research subjects can be divided into many elements enabling to make calculations nearly with few errors. For example, simulation of residual stress due to temperature influence at braking, according to "ABAQUS" program, presented on US government website [48], shows that calculation model of wagon wheel, particularly in rim part, is divided into hundreds of finite elements, that allowed to reach accurate orthographical stress diagrams distribution over a rim cross-section in the thermal crack occurrence area.

Numerous calculations of railway vehicle wheel pair, first of all wheel-axle assembly deflected mode, were fulfilled regardless of wheel pair elements interaction peculiarities, and the experiments are quite expensive. So, wheel calculations with all possible static and dynamic load combinations performed by Krivonogov V.G., (VNIIZhT), Vlaznev V.U., Potapov S.V. (MEI), were conducted on condition that over hub surface joined to car axle, building-in conditions were set (fixing in all three dimensions), that does not derogate obvious calculation advantages.

Purpose of this calculation is to determine reflected mode of wheel-axle assembly elements at various combinations of increased loading conditions and analysis of wheel-axle assembly bearing ability at high loading [49, 50].

How finite element analysis of contact zones was conducted? We should consider two bodies which are in contact [51]. Let us introduce dividing in finite elements for both bodies. We will call contact surface of one body active, and that of the other body - passive one, and the nodes placed on them active and passive accordingly. We should consider two nodes, we will call a - active node, p - passive node, $\vec{n}$ - normal vector to passive contact surface in node p. In the next iteration the nodes can take one of two positions shown on fig. 6.

In position a) nodes are not in contact before iteration process, in position b) nodes are in contact. The algorithm of node displacement determination is the following nodes displacements $\delta r_a'$, $\delta r_p'$ are determined from the equations: $A\delta r_a' = b_a'$, $B\delta r_p' = b_p'$, i.e. regardless of body contact interaction. Here A, B - are node stiffness matrices, b_a', b_p' - right-hand members of equations (1, 2).

We get: $\delta r_a' = \left(\delta u_a', \delta v_a', \delta w_a'\right)^T = A^{-1} b_a'$, $\delta r_p' = \left(\delta u_p', \delta v_p', \delta w_p'\right)^T = B^{-1} b_p'$. DNV variable is calculated (fig. 6a): $DNV = \left(\vec{r}_a' - \vec{r}_p'\right) \cdot \vec{n}$. Here $\vec{r}_a' = \vec{r}_a + \delta\vec{r}_a'$; $\vec{r}_p' = \vec{r}_p + \delta\vec{r}_p'$. If $DNV > 0$, nodes after such iteration are not in contact, their displacements get values: $\delta r_a = \delta r_a'$. By $DNV < 0$ nodes engage (fig. 6a) or stay in contact (fig. 6b). Then their displacements are calculated considering that there is no relative node sliding. Here we should distinguish between two cases. If nodes were in contact before iteration, in this case node displacements $\delta r_a''$ and $\delta r_p''$ are equal and determined by correlation: $\delta r_a'' = \delta r_p'' = \left(A + B\right)^{-1} \left(b_a' + b_p'\right)$. If nodes were not in contact before iteration, so $\delta r_a'' = \left(1 - ADD\right)\delta r_a' + \delta r_s$; $\delta r_p'' = \delta r_p' + \delta r_s$. Here $ADD = DNV / DD$; $DD = \delta r' \vec{n}_a$. Parameter ADD has meaning of displacement part $\delta r_a'$, falling within "implementation" of active node in passive area. Due to forces, exerting on node $p\left(b_p'\right)$, it displaces over $\delta r_p'$. Before engaging the node a travels a distance $\delta r_a'\left(1 - ADD\right)$.

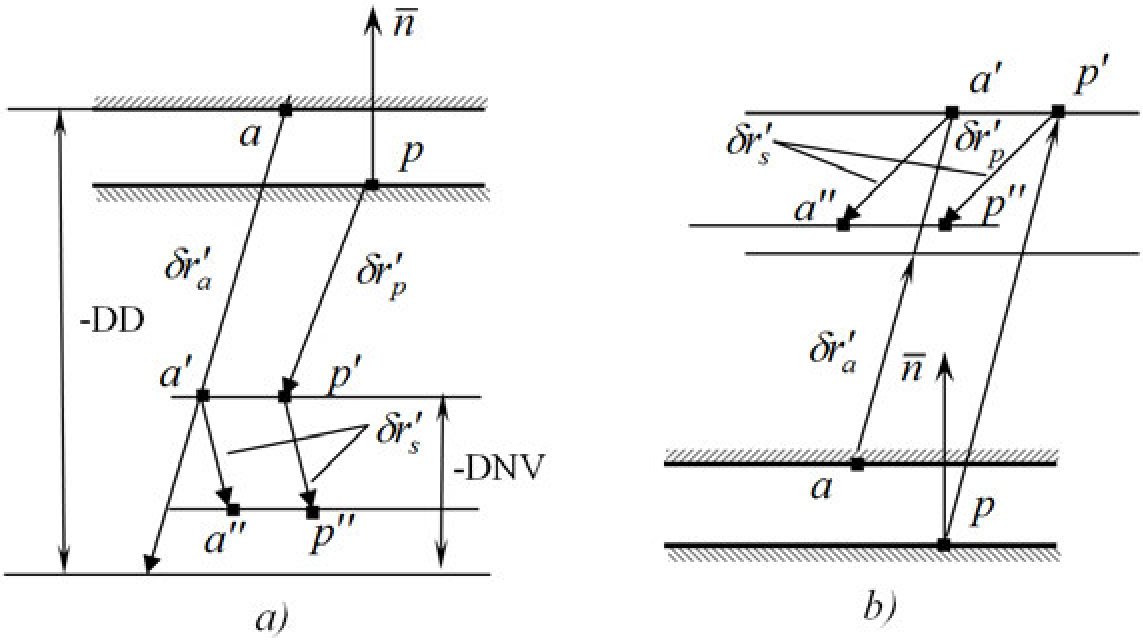

Fig. 6. Determination of relative displacement of contact points between two bodies
Rys. 6. Wyznaczenie względnego przemieszczenia punktów kontaktowych między dwoma ciałami

In this position it is exerted by force $b'_a ADD$. In the same position forces applied to node p are equilibrated. Further cooperative displacement of nodes over value $\delta r_s = (A+B)^{-1}(b'_a ADD)$ are determined. Then stiffness matrices are added (combined). Parameters when $ADD < 0$ have similar meaning. To solve problem of sliding we should determine reaction force in contact zone, i.e. the force which is applied by nodes a and p on each other. Assume $\vec{R}$ is force exerted on passive node. Correlation $A\delta r''_a = b'_a - R$, $R = A(\delta r'_a - \delta r''_a)$ is correct.

Normal and tangential components are the following: $\vec{R}_n = (\vec{R}\cdot\vec{n})\vec{n}$, $\vec{R}_\tau = \vec{R} - (\vec{R}\cdot\vec{n})\vec{n}$. Friction force limit value: $F_{fr} = fR_n$. There is no sliding when $|\vec{R}_\tau| \le F_{mp}$. Then for resultant displacements we have $\delta r_a = \delta r''_a$; $\delta r_p = \delta r''_p$.

If the condition $|\vec{R}_\tau| > F_{fr}$ is fulfilled, there is sliding of nodes. Let us consider sliding calculation model. Let us introduce coordinate system associated with the nodes. One axis is placed on the normal $\vec{n}$, two other – in the lines of unit vectors, tangents to contact surface. Node displacement vectors $\delta\vec{r}_{sa} = a_n\vec{n} + a_{\tau_1}\vec{\tau}_{\mathbf{1}} + a_{\tau_2}\vec{\tau}_{\mathbf{2}}$; $\delta\vec{r}_{sp} = a_n\vec{n} + b_{\tau_1}\vec{\tau}_1 + b_{\tau_2}\vec{\tau}_2$, or in matrix form: $\delta r_{sa} = a_n n + a_{\tau_1}\tau_1 + a_{\tau_2}\tau_2$; $\delta r_{sa} = a_n n + b_{\tau_1}\tau_1 + b_{\tau_2}\tau_2$. In these correlations it is assumed that in the normal direction node displacements are equal (a_n), and in the direction of osculating plane they are different. Displacements occur due to action of forces $b''_a = b'_a$ and $b''_p = b'_p$ or $b''_a = b'_a ADD$; $b''_p = 0$, as well as reaction force R and friction force F_{fr}. Let us introduce unit vector $\vec{e}$ in the direction of friction force. Then the passive node is exerted by force $\vec{F}_{fr} = fR\vec{e}$, and the active node – by opposite one. We should determine direction of vector $\vec{e}$ as follows. It is directed along relative node sliding vector which “is accumulated” on earlier done iterations:

$$\vec{e} = \frac{\vec{u}_\tau}{\|\vec{u}_\tau\|};\ \vec{u}_\tau = (\Delta\vec{r}_a - \Delta\vec{r}_p) - \left[(\Delta\vec{r}_a - \Delta\vec{r}_p)\cdot\vec{n}\right]\vec{n}.$$

Here $\Delta\vec{r}_a - \Delta\vec{r}_p$ is full displacement of node a to p, $\left[(\Delta\vec{r}_a - \Delta\vec{r}_p)\cdot\vec{n}\right]n$ - relative displacement in normal direction, therefore $\vec{e}$ - is unit vector in direction of tangential component of relative displacement, i.e. in direction of relative sliding.

Six values $a_n,\ a_\tau,\ a_{\tau_2},\ b_\tau,\ b_{\tau_2},\ R$ should be determined, i.e. five parameters which determine node displacements, and normal reaction value. To determine them we have: $A\delta r_{sa} = b''_a - R(fe+n)$; $B\delta r_{sp} = b''_p + R(fe+n)$. Here $e,\ n,\ \delta r_{sa},\ \delta r_{sp}$ are column-vectors of corresponding vectors coordinates relating to base coordinate system. We get:

$$(A_n)a_n + (A_{\tau_1})a_{\tau_1} + (A_{\tau_2})a_{\tau_2} + (fe+n)R = b''_a, \ (1)$$

$$(B_n)b_n + (B_{\tau_1})b_{\tau_1} + (B_{\tau_2})b_{\tau_2} + (fe+n)R = b''_p. \ (2)$$

Let us represent obtained expressions in form: $S_{\delta_x} = b$. Here $(a_n,\ a_\tau,\ a_{\tau_2},\ b_\tau,\ b_{\tau_2},\ R)^T$ is vector of unknowns, $b = \left(b''^{\tau}_a,\ b''^{\tau}_p\right)^T$ - vector of right members (forces), 6 x 6 matrix S is given by: $S = \begin{vmatrix} A_n & A_{\tau_1} & A_{\tau_2} & 0 & 0 & (fe+n) \\ B_n & 0 & 0 & B_{\tau_1} & B_{\tau_2} & (fe+n) \end{vmatrix}$. Simultaneous linear algebraic equations are solved by Gauss method of successive elimination. Displacements and reaction forces $R,\ F$ are determined. In case of sliding in a range of iterations the following case is possible: after performing of quite a lot of iterations displacement values are close to exact ones, the values δr_a and δr_p tend to zero, and forces tend to equilibrated values. Particularly: $R_n \to R$, $R_\tau \to fR$. Then by the next iteration correlation $R_\tau < fR_n$ can be performed, however by the previous iteration there was node sliding. In other words, in the case of exact solution we will get: $R_n = R,\ R_\tau = fR$.

Thus, if there was no node sliding by the last iteration, it does not guarantee, that there is no physical sliding between nodes. The value $\Delta R_\tau = |-R_\tau + fR|$ can cover such cases as node sliding factor. If $\Delta R_\tau \approx 0$, nodes are sliding. If ΔR_τ is rather bigger than zero, there is no sliding.

When studying wheel pair bearing ability, in particular wheel-axle assembly, the ratio of relative sliding areas (zones) and coupling areas of wheel hub points and axle wheel seat was determined. Simulation of wheel-axle assembly and half a wheelset, taking into account the axial symmetry is shown in fig. 7. All the calculations (more than 100 variants of various parameter combinations) were performed with program package RSFEM [49] as it allowed to determine size of wheel-to-axle contact surface, stress distribution in contact zone, zones of tight coupling or relative displacement (sliding) of contact points.

All the parameters except for temperature field varied in two levels. Temperature field - in three levels: no braking, service braking and emergency braking [50] (tab. 3).

Table 3

Levels of varying parameters

Vertical axle load	216 kN	245 kN	
Shearing force	60 kN	120 kN	
Torsional moment	0 kN·cm	1710 kN·cm	
Braking mode	0	1	2
Eccentricity of contact point with rail	2,8 cm	7,5 cm	
Wheel tread thickness	7 cm	2,2 cm	

Nonstationary thermal problem was solved to determine force factors at influence of irregular temperature field for wheel pair.

Two specific braking modes were selected according to [51].

1) Emergency braking of a car of mass 62 tones from speed 160 km/h to a stop, braking time 48 s. In this case heat flow delivered to wheel surface is 151,490 kW. In the work [51] it is equal to specific heat output of 680 kW/m^2.

2) Sustained braking when moving with constant speed of 60 km/h and operating time 1200 s. It corresponds to specific heat output of 177 kW/m^2 or heat flow of 39,432 kW.

Solution of nonstationary thermal problem by finite elements method is reduced to solution of differential equation [52]:

$$C \cdot \dot{T} + K \cdot T = -F \ ,$$

where C is heat capacity matrix,

K – heat conduction matrix,

F – node flow vector,

T – vector of required node temperatures.

Integration of this equation can be performed on the basis of finite-difference scheme. As result we get distributions at end-time points.

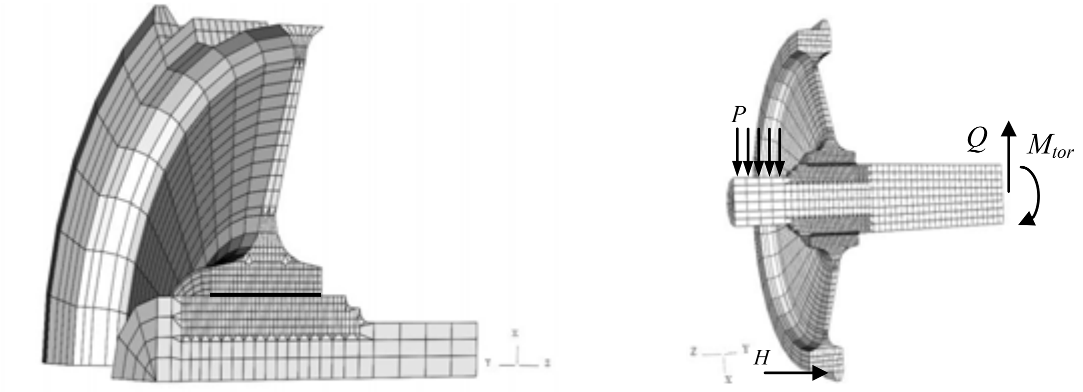

Fig. 7. Wheel-axle assembly model (static loads are shown)
Rys. 7. Model zestawu (pokazano obciążenia statyczne)

When calculating wagon wheel pair calculation model is applied, in the model finite element map in domain we are interested in is filled in substantially to get true picture of contact pressures, stresses, sliding direction, etc.

Basic wheel and axle dimensions of RF wagon wheel pair conform GOST 4835–80 and 4835–2006. Key factor to be determined is contact pressure distribution in wheel-axle assembly (i.e. in restricted area) and deflected mode in assembly.

8-, 6-, and 4-node finite elements were used when calculating. Altogether in calculation models 13741 nodes and 12301 elements were used for half-model and 26635 nodes and 25620 elements for calculation of whole wheel, the partition is quite exact (fig. 7). Material elastic behavior - Young's modulus of elasticity and Poisson ratio - were specified as follows: $E = 2 \cdot 10^6$ MPa, $\mu = 0{,}3$. Vertical load was distributed along axle neck nodes and axle inner face; shearing load was applied on wheel-to-rail contact point (constraining point); temperature field influence was considered by node forces application to all the nodes of calculation model (forces were applied everywhere, where temperature has raised for more than 1°C); torsional moment was applied on calculation model axle inner face of a wheel pair half like 4 forces [53].

Then some results of wheel pair calculation for worn out wheel rim of 2,2 cm thickness are presented, eccentricity of load application relative to wheel-axle assembly centre of 2 cm without torsional moment influence.

It should be noted that all the problems which take friction into account, have a lot of solutions. Distributions got are determined not only by loads, but also by load history. The results are one of possible variants of contact forces and stresses distribution.

On fig. 8, 9 diagrams are shown (wheel seat and axle neck models are shown) which represent distribution of contact pressure between wheel hub and wheel seat in wheel-axle assembly, but with various loads combination.

In the first case loads given really don't impact contact pressure symmetric property. The contact pressure has the greatest value – 77,7 MPa near the edges of the hub (see fig. 8). There was sharp rise of contact pressure in assembly to 130,7 MPa when high values of external loads, as well as pressure redistribution in assembly area, as shown in fig. 9. So moving with constant speed of 60 km/h and sustained braking during 1200 s brings to temperature rise on wheel thread more than 460^0C, and in wheel-axle assembly zone stresses are triple compared to first load variant (fig. 10).

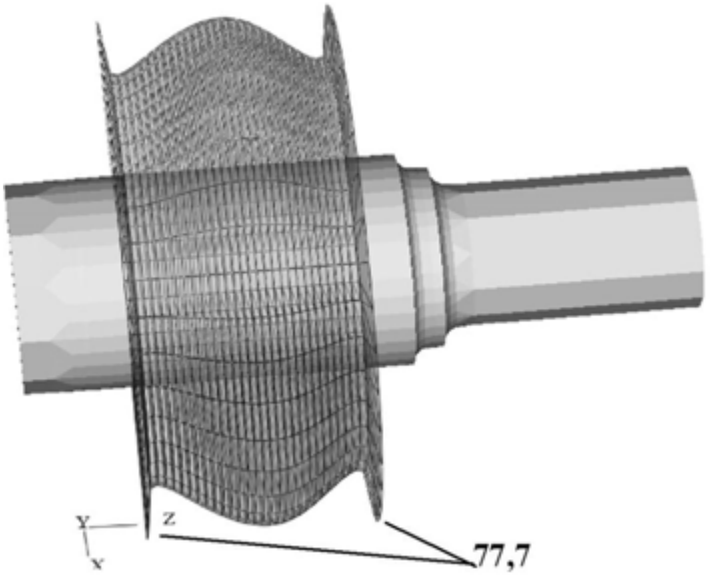

Fig. 8. Contact pressure distribution (MPa) in wheel-axle assembly with 0,2 mm interference; vertical load on wheel pair is 210 kN; horizontal rail reaction – load on wheel is 60 kN
Rys. 8. Rozkład naprężenia kontaktowego (MPa) w zestawie przy wcisku 0,2 mm; siła pionowa na zestaw jest równa 210 kN; pozioma reakcja szyny – siła przyłożona do koła wynosi 60 kN

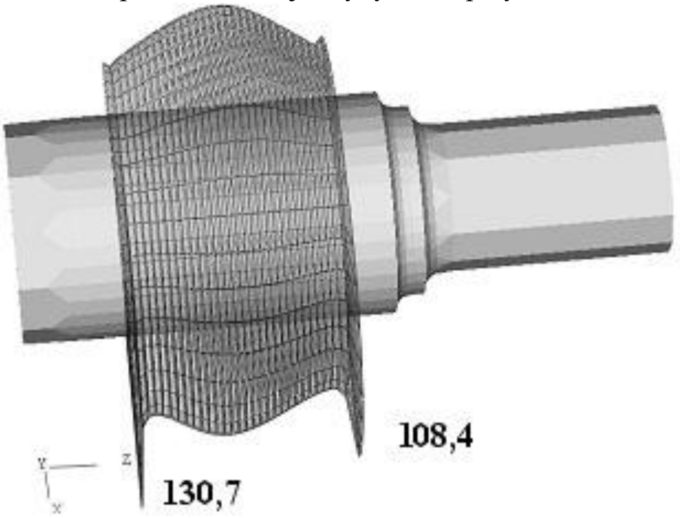

Fig. 9. Contact pressure distribution (MPa) in wheel-axle assembly with 0,2 mm interference; vertical load on wheel pair is 245 kN, horizontal rail reaction – load on wheel is 120 kN
Rys. 9. Rozkład naprężenia kontaktowego (MPa) w zestawie przy wcisku 0,2 mm; siła pionowa na zestaw jest równa 245 kN; pozioma reakcja szyny – siła przyłożona do koła wynosi 120 kN

However it constitutes no danger for bearing ability of wheel-axle assembly in terms of stressed state, as contact pressure values, and actually normal stresses, are far from critical values, as yield limit of wheel steel is $\sigma_y = 420$ MPa [53].

Obvious contact pressure redistribution in wheel-axle assembly zone is not dangerous in terms of stressed condition (fig. 11). But in this case space of direct and reverse sliding makes up 66%, what is the main reason on the part of deformed condition.

It is known [5] that if shearing stresses come up to value limits on the whole mating surface, assembly is broken, where mating surfaces displace relatively. There after numerous experiments friction coefficients are determined (average values): $f = 0{,}16$ when pressing out and $f = 0{,}1$ when stable motion after give. Taking into account average contact pressure in assembly $P = 60$ MPa, breaking shearing stress value should not exceed $\tau_{lim} = P \cdot f = 9{,}6$ MPa in average. However more than 50% of shear stress distribution (Fig. 10) have values higher than τ_{lim}.

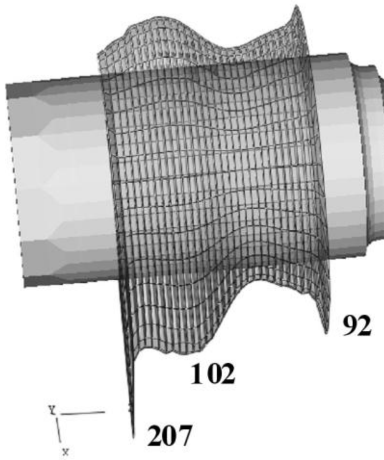

Fig. 10. Contact pressure distribution (MPa) in wheel-axle assembly under the same load conditions with regard to temperature influence

Rys. 10. Rozkład naprężenia kontaktowego (MPa) w zestawie przy oddziaływaniu tych samych warunków brzegowych i uwzględnieniu szczątkowych termicznych naprężeń

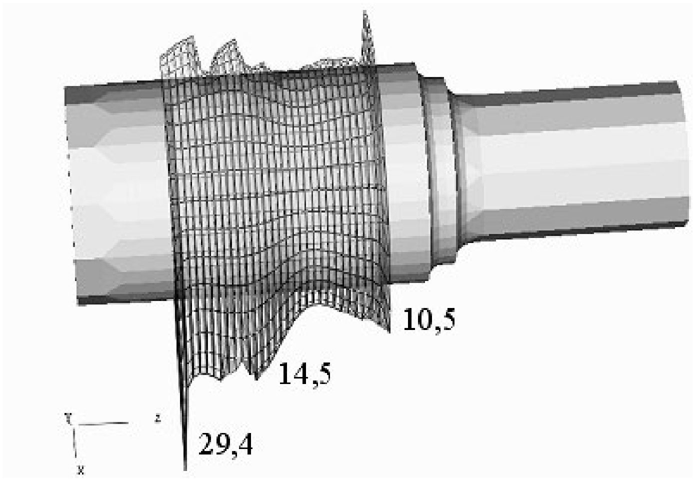

Fig. 11. Distribution of shear stresses (MPa) in wheel-axle assembly with same boundary conditions under the temperature influence

Rys. 11. Rozkład naprężenia kontaktowego (MPa) w zestawie przy oddziaływaniu tych samych warunków brzegowych i uwzględnieniu obciążenia termicznego

Sliding zone distribution, shown on fig. 12, is obtained by correlation of shear stresses to normal ones. So, distribution's flat areas point to zones of wheel-axle contact points relative sliding, here shear stresses are of considerable values (see fig. 11). Values of the most displacements (mm) are shown in characteristics – end cross-sections and on wheel thread. The largest sliding forward and reverse direction is observed at the assembly edges and may travel a considerable distance from the contact area of wheel and axle.

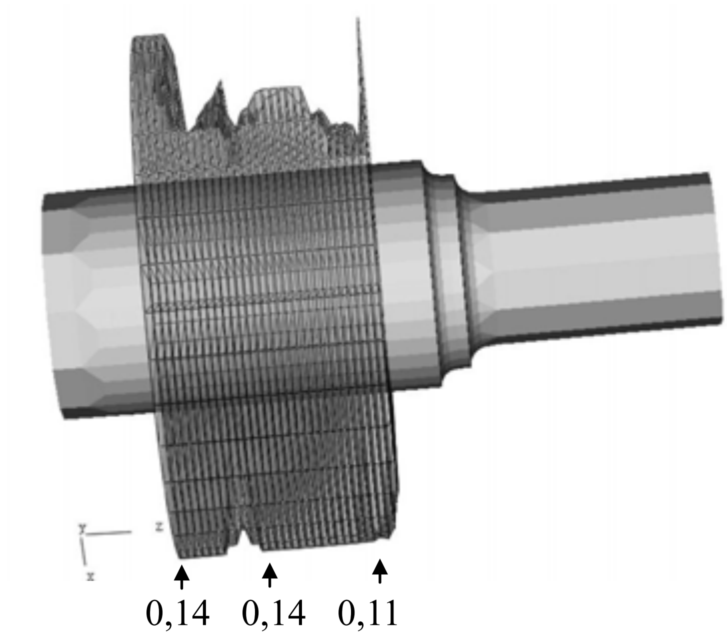

Fig. 12. Sliding zones pattern in wheel-axle assembly under the same loading conditions with regard to temperature influence
Rys. 12. Strefy poślizgu koła względem osi przy tych samych warunkach obciążenia w odniesieniu do wpływu temperatury

In the work [3] when performing physical full-scale experiment on determination of absolute deformations in wheel seat and wheel hub it was recommended to consider the contact as fixed when deformation difference less than $10 \cdot 10^{-6}$ mm. In the same work [6] only fixed contact zones shear strength was taken as tolerable exploitation durability. Under such complicated load conditions over more than a half of nominal contact space of wheel seat and wheel hub nodes relative displacement value ranges from $5 \cdot 10^{-4}$ mm along Y-axis to $7 \cdot 10^{-4}$ mm along Z-axis and to 0,19 mm (when 0,2 mm interference) along X-axis.

Theoretical calculation results of sliding and mating zones according two-dimensional assembly model [23], obtained by us, shows that when axle loading $P = 245$ kN direct and reverse sliding space in contact zone comes up to 55%. By various combinations of six load factors (complete factorial experiment) more than in 10% of load variants sliding and mating zones space in contact zone exceed 50% of wheel-axle contact area [54]. Considering dynamic loading, stress relaxation, fretting-corrosion it can bring to assembly's crippling. Therefore more attention should be paid to wheel-axle durability in operation, as it is done at present time, considering tendencies to load operational conditions stiffening.

It is possible to prevent wheel-axle assembly dangerous condition in operation, when applying obtained data base as comparative one to loading operating parameters – vertical and horizontal load, thermal influence due to braking, wheel pair position on rail-track, wheel rim thickness and so on, which can be easily obtained by known wheel pair control units.

Here are some conclusions obtained by the solutions.

1. Vertical load $P = 245$ kN/axle does not bring to dangerous deflected mode of wheel-axle assembly.
2. Increasing of horizontal load up to $Q = 120$ kN brings to contact pressures and tangential (shearing) stresses redistribution in assembly, and consequently to increase of contact points relative sliding zones.

3. In variants with temperature influence due to braking, in addition to mentioned, wheel-axle contact points relative sliding zones achieve substantial values.

Deflected mode of not only wheel-axle assembly, but also of wheel disk and its rim is determined due to performing of complete factorial experiment.

Deflected mode of wear out wheel disk due to horizontal load impact $Q = 120$ kN is shown on fig. 13. Other parameters have minimal values. Stresses zones of different levels are restricted by isolines. Here values of von Mises equivalent stress are far from limit values and make up $\sigma_{equ} = 266$ MPa.

On fig. 14 wheel rim is shown for load case when $P = 245$ kN, $Q = 120$ kN. Here when emergency braking equivalent stresses $\sigma_{equ} = 575$ MPa are realized in disk-to-rim transition zone. Loads in taping line zone also exceed wheel steel flow limit substantially and are $\sigma_{equ} = 702$ MPa.

Fig. 15 represents impact of sustained (during 2 minutes) service braking by speed of 60 km/h. Taking into account influence of other force factors ($P = 245$ kN, $Q = 120$ kN) maximal equivalent stresses in disk-rim mating zone make up more than 957 MPa. As well as stresses on wheal thread are high enough – 1000 MPa. Values of these stresses almost reach

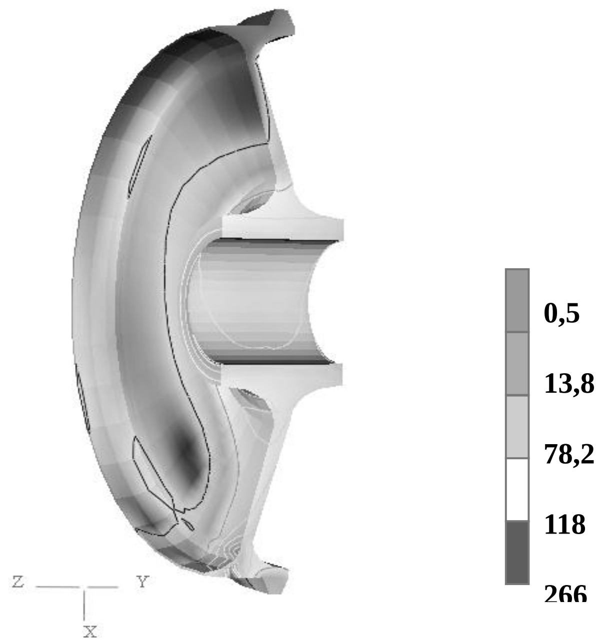

wheel steel limit strength $\sigma_{equ} = 1100$ MPa.

Fig. 13. Stresses in wheel disk due to high horizontal load $Q = 120$ kN

Rys. 13. Naprężenia tarczy koła przy oddziaływaniu dużej siły poziomej $Q = 120$ kN

Given illustrations how negative temperature impact when various braking modes and high horizontal load for thin rim. However such impact is the same for new wheel. It is no wonder that occur such defects like “galling”, “thermal pit breaches” or wheel disk cracks in disk-rim transition zone.

As the biggest attention in this research is paid to wheel-axle assembly, it should be noted that sliding zones value exceeded 50% of 96 variants in 10% cases. This value can’t guarantee wheel-axle assembly durability and consequently traffic safety.

On figures only individual cases of calculation results are shown when more than one hundred initial parameters combination variants – external influences and geometrical parameters. Obtained calculation results give more than fifty parameters, by which not only wheel-axle deflected mode can be estimated, but also bearing ability of the assembly.

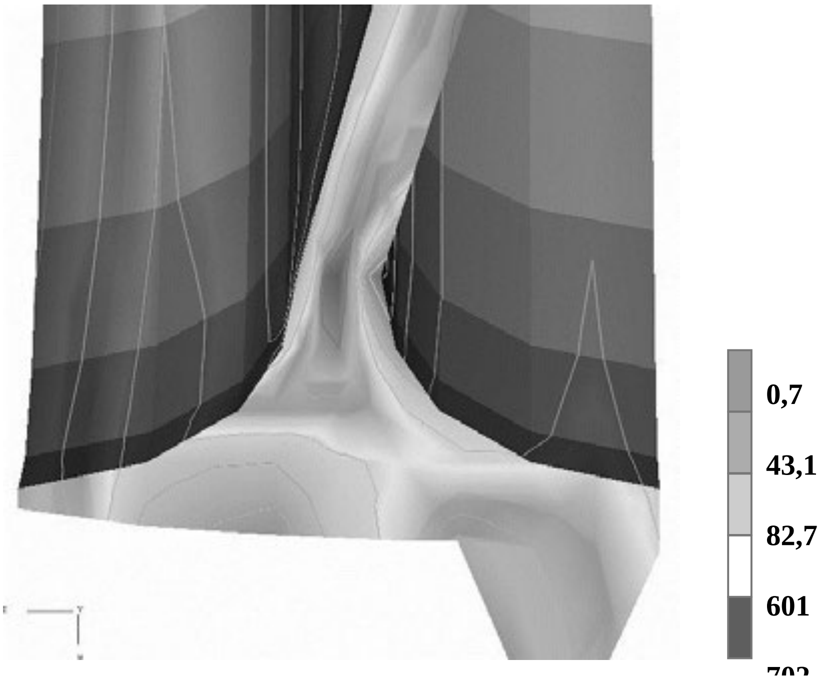

Fig. 14. Stresses near thin wheel rim due to high horizontal load $Q = 120$ kN and emergency braking

Rys. 14. Naprężenia w strefie cienkiego wieńca powstałe wskutek dużej siły poziomej $Q = 120$ kN i nagłego hamowania

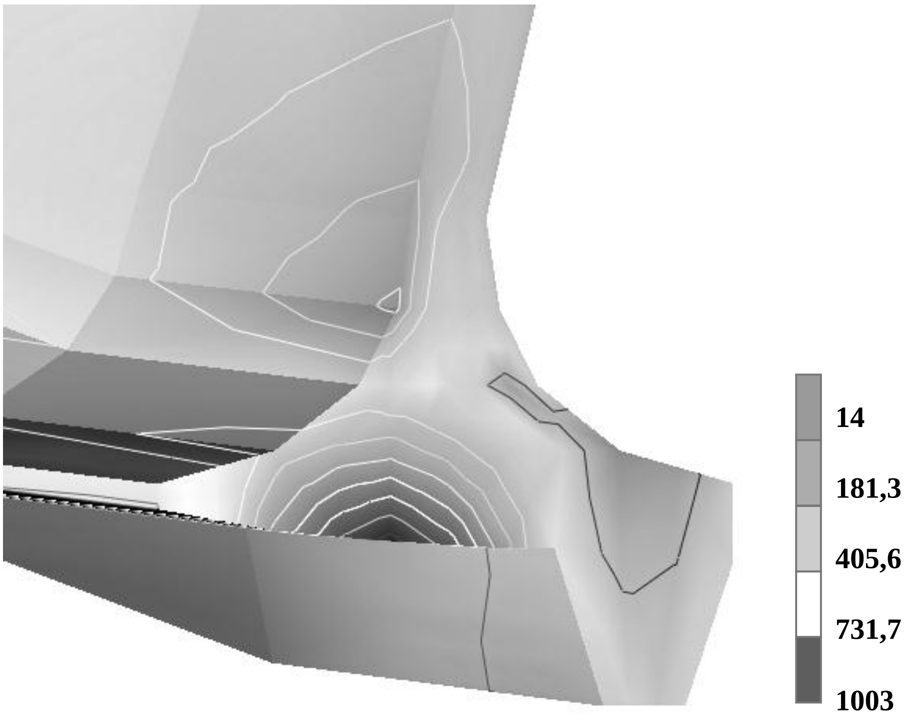

Fig. 15. Stresses near thin wheel rim due to high horizontal load $Q = 120$ kN, vertical load $P = 245$ kN and sustained braking

Rys. 15. Naprężenia w strefie cienkiego wieńca powstałe wskutek dużej siły poziomej $Q = 120$ kN, pionowej siły $P = 245$ kN i trwałego hamowania

Fundamental conclusions when studying wheel pair deflected mode are the following.

The most negative impact on wheel-axle deflected mode generates temperature influence due to braking, where sustained (service) braking is more dangerous.

Vertical load growth, availability of torsional moment, eccentricity of vertical load application do not generate any substantial negative impact, stresses don’t reach significant values.

Negative horizontal load – rail reaction has an impact, especially combined with above mentioned loading factors.

In terms of distribution of dangerous stresses over wheel rim unworn wheel has the advantage compared to wheel with thin rim.

What about wheel-axle assembly, so horizontal load and the most negative factors combination, selected for research, generate dramatic impact on sliding zone value in assembly, what reduces assembly’s durability.

In conclusion it should be noted that wheel pair deflected mode calculation results involve very much, each material for further researches with mathematical statistics method. Contact pressure value and distribution, shearing and normal components of stress, relative displacements and deformations of wheel hub and wheel seat are influential parameters of sliding and mating zones value in wheel-axle assembly [56].

It can be multiple regression analysis, where when choosing as response function, for example, sliding and mating zones value in wheel-axle assembly, depending of the quantity of initial calculation parameters (here – six), we can obtain any identical regression equations, which correspond to adequate measures. Obtained results can be applied in wheel pair monitoring system when in operation, using modern measurement instrumentation [55], which register load value, temperature influence, wheel pair geometrical parameters etc.

It can be multi-component or factor analysis [56], where wheel pair and wheel-axle assembly bearing ability are categorized by five-six consolidated indexes, interpreted through correlate matrix rotation with a lot of wheel pair bearing ability indexes.

One of the competent instruments of statistical investigations is discriminatory analysis, which application when studying wheel-axle assembly bearing ability is explained in the next part.

5. APPLICATION OF DISCRIMINANT ANALYSIS WHILE INVESTIGATING BEARING ABILITY OF PRESS ASSEMBLY OF WAGON WHEELSET

Traditional theoretical calculations of wheel pairs strength include three main stages: determination of operation forces and choice of calculation model, stress and deformation calculation and strength evaluation according to relevant criteria. Practical application of numerical methods provides such possibility [58].

While studying stress state of wheel pair elements we have investigated mating with wheel fit and axle specifying assembly strength.

On fig. 16 we can see distribution of slide zones in wheel and an axle press assembly of modern wheelset of the Russian railways at vertical axle load 250 kN, horizontal - 60 kN (one of the variants).

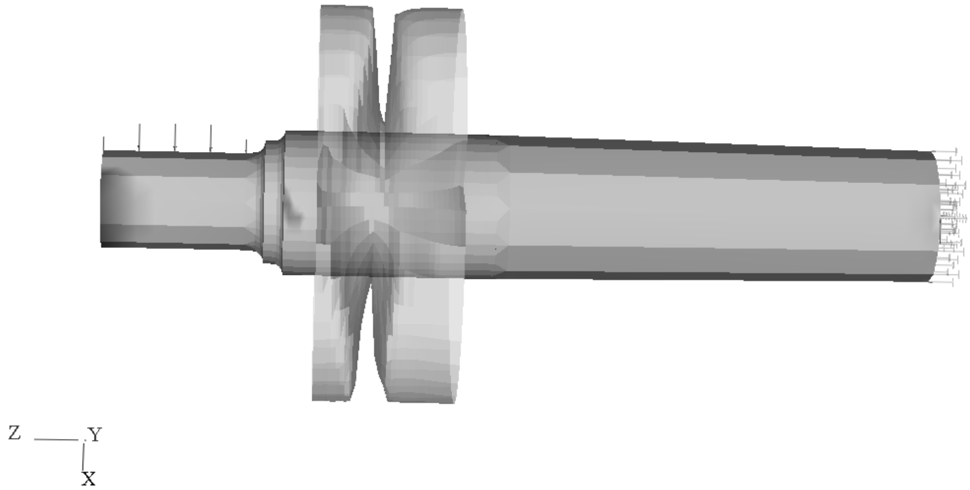

Fig. 16. Diagram of slide zones in wheel and axle assembly (half an axle)
Rys. 16. Schemat stref poślizgu pomiędzy kołem a osią w zestawie (pokazano połowę zestawu)

Evaluation of effect of load factors, wheel pair configuration, physical and mechanical properties of a wheel and an axle, mating in a press assembly seems difficult for the following reasons. Slide and coupling area is not liable to measuring, especially at dynamic loading but some wheel pair loading parameters can be measured. It is also possible to classify assembly reliability degree by means of discriminant analysis with due account for available results of calculation of stress and deformation state of wheel pair and its press assembly.

The main objective of discriminant analysis is to work out a rule enabling to assign a specific element to one of *k* groups $W_1, W_2, \ldots, W_k$ on the basis of measurement (calculation) of p parameters $x_1, \ldots, x_p$. Classification procedure in case of p continuous variables assumes that investigations belong to one of populations having multidimensional normal distributions. To answer the question to which of these populations to relate new values of the investigated parameter according to the available information it is necessary to choose such linear combination of variables called discriminant function that would divide groups

$$z = \alpha_1 x_1 + \alpha_2 x_2 + \ldots + \alpha_p x_p ,$$

where $\alpha_1, \ldots, \alpha_p$ - some constants minimizing probability of misclassification, it is possible to choose them and show that classification procedure is successful enough [59]. If *x* result arrives at W_1, *z* value has normal distribution with average $\xi_1 = \sum_{j=1}^{p} \alpha_j \mu_{1j}$ and dispersion $\sigma_z^2 = \sum_{i=1}^{p} \sum_{j=1}^{p} \alpha_i \sigma_{ij} \alpha_j$. Similarly for *x* referred to W_2, *z* size has normal distribution with average $\xi_2 = \sum_{j=1}^{p} \alpha_j \mu_{2j}$ and with the same dispersion σ_z^2 . It is reasonable to choose such $\alpha_1, \ldots, \alpha_p$ that ξ_1 and ξ_2 would be as much separated as possible from each other with respect to σ_z^2. For this purpose Mahalanobis distance $\Delta^2 = \frac{(\xi_1 - \xi_2)^2}{\sigma_z^2}$, the value measuring distances between populations, is used. Thus, $\alpha_1, \ldots, \alpha_p$ should maximize Δ^2. Upon receiving α_i , value of discriminant function is assigned to each object $x_1, \ldots, x_p$ [59].

When calculating bearing ability of wagon wheel pair, its press assembly in particular, one of the following objective of discriminant analysis may occur. Upon carrying out full factorial test values of slide and coupling zones in assembly for 96 loading variants are determined [50]. For classification value of slide zone in press assembly is subdivided in three subgroups: less than 20 % - subgroup with high degree of assembly reliability, from 20 % to 40 % - subgroup with medium reliability, over 40 % (in calculation results and more than 60 %) - subgroup with a low degree of reliability. Then by means of discriminant analysis methods the linear combination of variables leading to this or that reliability group in our terminology is determined. In fact we get formulas for determination of slide zones values, due to them it is possible to determine assembly reliability with specific accuracy degree in the result of, for example, measurements on the basis of diagnostic equipment applied in modern operation conditions – for strain measurement, determination of wheel temperature and wear etc, without damage to assembly.

The following procedure is carried out: grouping variable is selected, in this case, variable «slide zone», as well as six mutually independent variables which variation levels do not have effect on one other: vertical load on wheel pair (designation VERT), horizontal reaction of a rail - transverse load (POPER) applied to wheel rim, temperature effect due to interaction of a wheel and a brake shoe (TORM), torque due to uneven brake shoes pressing to pair wheels (MOKR), eccentricity of application of rail vertical reaction with respect to central cross section of wheel and axle press assembly (EXCENT), size of taping line set by the parameter – wheel rim thickness (TOLOBOD) [50, 54].

Variable «slide zone» is coded. If slide zones value is less than 20%, «*b*» index is assigned to this group of values; if slide zones value is more than 20% but less than 40%, «*c*» index is assigned to this group of values; if slide zones value is more than 40%, «*d*» index is assigned to this group of values. Indexes are coded by computer as follows: «*b*» =100, *«c»* =101, «*d*» =102 [58].

It is possible to apply step by step discriminant analysis to obtain a classification model using Fisher's statistics of inclusion or exclusion – tab. 4. According to it such variables as vertical load, wheel rim thickness or temperature effect can be excluded from model for specific initial criteria, but for physical reasons it is necessary to keep them. It is common knowledge that crossheads appeared due to wheel braking and seizure can overload a wheel pair to 40-45 tons**,** but there were cases of load amount fixing 79 tons. It also refers to other variables. Wilks' Lamda values fall within the limits of [0,1], in this case it is possible to state that discrimination ability is 50 %. Tolerance shown in the table represents 1 minus square of multiple correlation of the specific variable with other variables in the model. In this case all variables are included in the model as they have high tolerance.

To test the hypothesis H_0 : $\Delta^2 = 0$ meaning equality of the averages in groups: H_0 : $\mu_1=\mu_2=\mu_3$: value of F - statistics: $F(12,179) = 6,058$ meaning $p < 0,001$.

Tab. 5 shows classification functions for three groups of slide zone areas. The classification functions represent formulas by which it is possible to calculate classification criteria for new cases.

Thus, discriminant function describing variables combination resulting in appearance of slide zones their size being up to 20% of press assembly area, is as follows:

$$b(10) = -132{,}552 + 1{,}0691 \cdot VERT + 0{,}1094 \cdot POPER + 0{,}0014 \cdot MOKR +$$
[illegible]

Table 4

Summary: variables in the model

N=9	Discriminant Function Analy No. of vars in model: 6; Gro Wilks' Lambda: ,500 ,0740 app Wil Lan	Par Lan	F-re (2,8	p-le	Tol	1-T (R-S
VEF	0,51	0,97	1,2:	0,2	0,98	0,01
POF	0,67	0,74	14,9	0,00	0,92	0,07
MOK	0,57	0,87	6,34	0,00	0,98	0,01
TOF	0,52	0,95	1,9	0,14	0,99	0,00
EXC	0,63	0,78	12,2	0,00	0,92	0,07
TOL	0,53	0,94	2,71	0,07	0,97	0,02

Table 5

Classification functions for grouping variable ZSKOL

Variab	Classification Functions b p=,302	c p=,541	d p=,156
VERT	1,069	1,095	1,112
POPE	0,109	0,1519	0,182
MOKF	0,001	0,000:	0,001
TORM	0,010	0,009:	-0,000
EXCE	0,807	0,253	0,031
TOLO	0,625	0,419	0,248
Const	-132,5:	-136,1	-142,9

When the size of slide zones is from 20 % to 40 % of press assembly area

$$c(10) = -136{,}165 + 1{,}0956 \cdot VERT + 0{,}1519 \cdot POPER + 0{,}0003 \cdot MOKR +$$
[illegible]

If the size of slide zones is above 40 % of press assembly area, discriminant function is as follows:

[illegible]

To evaluate bearing ability of wheel and axle press assembly for new loading conditions it is necessary to insert variables values into formulas and calculate classification values of slide zones in codes and refer them to a relevant group - «*b*», «*c*», «*d*». Slide zones size will belong to such a class for which classification value is maximum.

We should determine squared Mahalanobis distances to group centroids specifying different reliability degrees of press assembly.

The case should cover the group to which selected Mahalanobis distance is minimum. We should determine probability of calculated slide zone area belonging to different groups.

Each case under consideration covers the group with maximum posterior probability. Tab. 6 and 7 are shown fragmentarily – full tables contain 96 classifications.

Table 6

Squared Mahalanobis distances to groups «*b*», «*c*», «*d*»

Cas	Squared Mahalanobis I Incorrect classifications Obse Clas	b p=.3	c p=.5	d p=.1
*	b	7,4	5,6	9,3
*	b	9,1	5,3	7,4
	b	4,7	8,1	13,
	b	5,5	6,9	11,
	c	8,0	6,7	13,
	c	9,4	6,1	11,

Table 7

Probability of slide zone area belonging to groups «*b*», «*c*», «*d*»

Cas	Posterior Probabilities Incorrect classifications ar Obser Class	b p=,30	c p=,54	d p=,15
*	b	0,182	0,782	0,035
*	b	0,070	0,841	0,088
	b	0,756	0,239	0,003
	b	0,520	0,462	0,017
	c	0,228	0,763	0,008
	c	0,094	0,883	0,021
	b	0,801	0,197	0,000

Thus, for possible loading conditions VERT=300 kN/axle, POPER=160 kN, TOLOBOD=2,2 cm, MOKR=0, EXCENT=2,8 cm, TEMP=39,44 kW (heat flow at sustained braking – [51]) Mahalanobis distances from new supervision to group centroids

Supervision	*b*	*c*	*d*
---	**53,67793**	**37,27156**	**31,03219**

show minimum value for group «*d*». Posterior probabilities are equal

Supervision	*b*	*c*	*d*
---	**0,000020**	**0,132790**	**0,867190**

New supervision with probability 0,867 covers group «*d*». Under these loading conditions assembly bearing ability will have low reliability.

To increase discrimination level one can choose any weight variable enabling to set weight for various cases (proportionally to variable values). While determining, for example, «TORM» variable as weight one, Wilks's Lambda parameter becomes equal to 0,37 with relevant statistics $F(12, 12208) = 649{,}14$ at $p < 0{,}0001$, thus it is possible to speak about higher discrimination degree.

Division of press assembly calculation results shown on fig. 17 in the form of percentage ratio of slide zones area is given for two groups – with slide zone area less than 20% and more than 40% of total area of wheel and axle mating.

Fig. 17 shows division of populations with high reliability degree of «*b*» assembly and with low reliability degree of «*d*» press assembly.

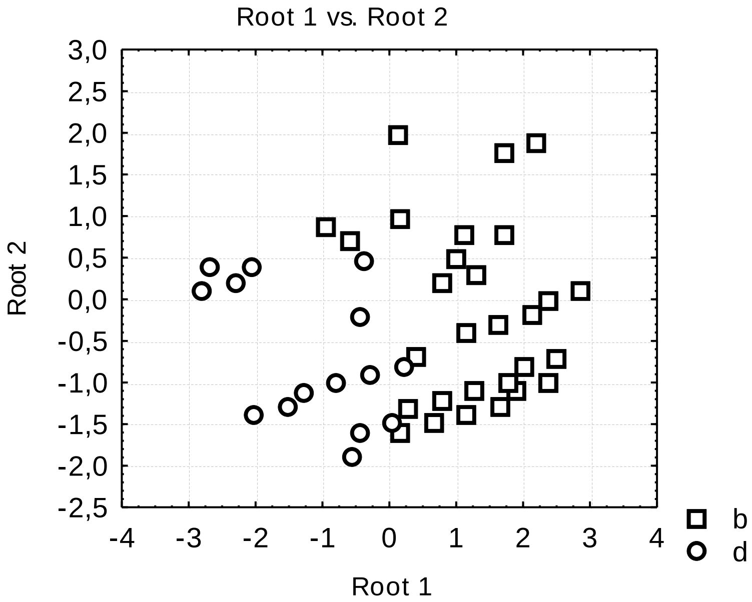

Fig. 17. Diagram of canonical values dispersion (division of reliability degrees)
Fig. 17. Diagram rozproszenia kanonicznych wartości (podział stopni niezawodności)

As initial variables parameters can be measured while wheel pair moving [55], it is possible to evaluate wheel pair press assembly reliability at its operation using data bank of wheel and axle press assembly calculation as well as classified intervals of slide zone areas by means of discriminant analysis.

Main conclusions are as follows. According results of calculation of stress-deformed state wheelset using discriminant analysis techniques can be classified as bearing ability wheel-axle assembly. Knowing values of these parameters in the system for monitoring the wheelset-to-use, and using the resulting database of calculating stress-deformed state wheelset, as a comparison, one can detect wheel sets with a large area of slide bands that threaten safety.

REFERENCES

1. Shkolnik L.M.: Increasing of railway rolling stock axle strength. Transport, Moscow, 1964
2. Andreev G.Ya.: Wheelset elements, during its thermal assembly. Kharkov University Publishers, Kharkov 1965.
3. Naumov I.V., Martynov N.I., Gudkov V.N.: Strength of pressure assemblies and stresses of car wheel pair elements. ZNII MPS (VNIIZhT), Ed. 384. Transport, Moscow 1969.
4. Berniker E.I.: Pressure Fittings in Machine Building. Mashinostroenie, Moscow 1966.
5. Grechischev E.S., Ilyashenko A.A.: Interferences. Mashinostroenie, Moscow 1981.
6. Serensen S.V., Kogaev V.P., Shneiderovich R.M.: Bearing Capacity and the Strength Calculation of Machines. Mashinostroenie, Moscow 1975.

7. Krotov S.V.: Wheel pair forming quality analysis. [In:] Increase of operational reliability of locomotives and its use improvement. Interacademic subject collection. RIIZhT, Rostov-on-Don, 1982, p. 94-95.
8. Veller V.A., V.A. Grechischev E.S., Rogozhina A.E.: Increase of railway rolling stock wheel strength. Transzheldorizdat, Moscow 1963.
9. Classification of wheel pair and wheel pair elements defects ITM1-B. Transport, Moscow, 1978.
10. Frenkel V.Ya., Kozlova M.A., Flumenbaum S.Kh.: Research of design factors of next-generation freight car wheel pair [In:] Car parameters determination. Analysis of units and equipment structure/ Edited volume BNII of car-building. Transport, Moscow 1985, p. 66-74.
11. Instruction on check-up, examination, repair and formation of wheel sets ZV/3429 MPS. Transport, Moscow 1977.
12. Bobrovnikov G.A.: Strength of Force Fits Attained by Cooling. Mashinostroenie, Moscow 1975.
13. Waterhouse R.B.: Fretting-corrossion. Mashinostroenie, Leningrad 1976.
14. Evdokimov Yu. A., Kolesnikov V.I.: Planning and analysis of experiments at solution of friction and deterioration problems. Nauka, Moscow 1980.
15. Lazaryan V.A.: Wagon dynamics. Transzheldorizdat, Moscow 1964.
16. Duvalyan S.V.: Analytical determination of stresses in all-rolled wheel disk. Vestnik VNIIZHT, No. 3, 1960, p. 36-40.
17. Shevchenko P.V.: Research on the buildup of cracks in railway wheel pair axles and measures for their strength and life-time improvement. KhIIT, Kharkov 1964.
18. Savvushkin E.S.: Contact pressure distribution in wheel hub and axle when press fitting. Vestnik VNIIZHT, No. 1, 1958, p. 49-53.
19. Nikolsky E.N.: Analysis of algorithms, obtained by combined application of primary systems alternation method and finite element method. [In:] Car body structural mechanics issues. Tula polytechnic Institute, Tula 1978, p. 4-13.
20. Sakalo V.I.: Solution of railway rolling stock application contact problems by finite element method. BITM, Bryansk 1986.
21. Podlesnov Yu.P., Sakalo V.I., Khudyakova G.A.: Finite element relaxation method for elasticity theory application problems. [In:] Reliability and dynamics research issues of transport machines and railway rolling stock elements. TPI, Tula 1979, p. 96.
22. Savchuk O.M., Pasternak N.A.: Research of hollow wagon axle-wheel assembly. Vestnik VNIIZHT, No. 2, 1979, p. 28-31.
23. Krotov S.V.: Internal forces and displacements in axle and wagon wheel hub. [In:] Dynamics, strength and reliability of transport machines. BITM, Bryansk 1990, p. 92-101.
24. Biderman V.L.: Structural damping in force fit elements. [In:] Strength calculations. Mashinostroenie, No.19, Moscow 1978, p. 3-10.
25. Barlow J.: Constraint Relationships in Linear and Nonlinear Finite Element Analyses. International Journal for Numerical Methods in Engineering, Vol. 18, 1982, p. 521-533.
26. Bathe K.-J.: Finite Element Procedures. Prentice Hall, Englewood Cliffs, NJ 1996.
27. Void H.: Substructure Analysis with Linear Constraints Using Natural Factor Formulation. Computer Methods in Applied Mechanics and Engineering, Vol. 10, 1977, p. 151-163.
28. Heegaard J.-H., Curnier A.: An Augmented Lagrangian Method for Discrete Large-Slip Contact Problems. International Journal for Numerical Methods in Engineering, Vol. 36, 1993, p. 569-593.
29. Felippa C.A.: Error Analysis of Penalty Function Techniques for Constraint Definition in

Linear Algebraic Systems. International Journal for Numerical Methods in Engineering, Vol. 11, 1977, p. 709-728.
30. Webb J.P.: Imposing Linear Constraints in Finite Element Analysis. Communications in Applied Numerical Methods, Vol. 6, no. 6, 1990, p. 471-475.
31. Zhong Z.-H.: Finite Element Procedures for Contact-Impact Problems. Oxford University Press, 1993.
32. Zhu J.Z., Zienkiewicz O.C.: Adaptive Techniques in Finite Element Method. Communications in Applied Numerical Methods, Vol. 4, 1988, p. 197-204.
33. Zienkiewicz O.C., Zhu J.Z.: Adaptivity and Mesh Generation. International Journal for Numerical Methods in Engineering, Vol. 32, 1991, p. 783-810.
34. Kiylo O.L.: Simulation and study of interference assemblies of structural elements rotor retained units of turbo-alternators. St. Petersburg 2003.
35. ANSYS. Basic Analysis Procedures Guide. Rel. 6.0. ANSYS Inc., Huston 2002.
36. Parsons B., Wilson E.: A method for determining the surface contact stresses. In: ASME works. Ser. Design & Technology, Vol. 92, 1970, p. 293-303.
37. Lurye A.I.: Three-dimensional elasticity theory problems. Gostekhizdat, Moscow 1955.
38. Iosilevich G.B., Lukaschuk Yu.V.: Stress distribution in assemblies with guaranteed interference. Vestnik mashinostroeniya, No.6, 1979, p. 25-26.
39. Sherman D.I.: About stressed state of some pressed parts. Izvestiya AN USSR. OTN, No. 9, 1948, p. 1371-1388.
40. Tarabasov N.D.: Calculation of wringing fits in machine building. Mashgiz, Moscow 1961.
41. Krotov S.V., Gavrilov S.K., Krotov V.P.: Stressed state calculation of compound cylinder in conformity of known contact pressure. Daghestani Scientific Center Bulletin, No. 19, 2010, p. 27-35.
42. Ekberg A.: Fretting fatigue of railway axles - a review of predictive methods and an outline of a finite element model. IMechE Journal of Rail and Rapid Transit. No. 218, 2004, p. 299-316.
43. Waterhouse R.B.: Fretting fatigue. Int. Mater. Rev., No. 37, 1992, p. 77–97.
44. Fellows L.J., Nowell D., Hills D.A.: On the initiation of fretting fatigue cracks. Wear, No. 205, 1997, p. 120–129.
45. Vingsbo O., Soderberg D.: On fretting maps. Wear, No. 126, 1988, p. 131–147.
46. Sitarz M., Sladkowski A., Bizon K., Chruzik K.: Designing of railway wheels. Part 1: Finite element method. Proceedings of the Institution of Mechanical Engineers, Part F: Journal of Rail and Rapid Transit, Vol. 219, No. 2, 2005, p. 91-110.
47. Annual report, Safety statistics. Federal Railroad Administration, USA, 30.06.2006, http://www.fra.dot.gov
48. Residual stresses in railroad commuter car wheels/Research results RR99-01. US Department of Transportation, Federal Railroad Administration Research Results, USA 1999. http://www.fra.dot.gov/downloads/research/rr99_01.pdf.
49. Sakalo V.I., Olshevsky A.A., Shevchenko K.V.: RSFEM Program Package for Contact Units Investigation. Consideration of Railway Transport Problems, Proc. of Conf. „Railway Bogies and Running Gears”, Budapest 2001, p. 162-164.
50. Krotov V., Krotov S.: Estimate the carrying capacity of the wheelset at high loads. Bulletin RGUPS, No. 1, 2005, p. 35-38.
51. Kiselev S.N., Inozemtsev V.G., Petrov S.Yu., Kiselev A.S.: Temperature fields, deformations and stresses in all-round wheels when various braking modes. Vestnik VNIIZHT, No. 7, 1994, p. 13-17.
52. Segerlind L.: Application of finite element method. Mir, Moscow 1979.
53. Krotov S.V., Krotov V.P.: Analysis of wagon wheel pair pressing assembly bearing ability

with finite element method. Vestnik IrGTU, No.7 (47), 2010, p. 32-35.
54. Krotov S.V., Krotov V.P.: Influence of increasing of loading conditions on wagon wheel pair pressing assembly bearing ability. Vestnik transporta Povolzhya, No.4 (24), 2010, p. 32-35.
55. Shenck process. Wheel load diagnostic and testing systems. MULTIRAIL train weighing and monitoring - one solution - multi-purpose. http://www.schenckprocess.com/.
56. Krotov V., Krotov S.: Application of the method of the principal components for the analysis of bearing ability of the wheel pair of the car. Transport Problems, Vol .4, No. 4, 2009, p. 15-25.
57. Sladkovsky A., Yessaulov V., Shmurygin N., Taran Y., Gubenko S.: An Analysis of Stress and Strain in Freight Car Wheels. [In:] Computational Method and Experimental Measurements VIII. Computational Mechanics Publications, Southampton, Boston 1997, p. 15-24.
58. Krotov S., Krotov V.: Application of the discriminant analysis at research of bearing ability of the wheel pair of the car. Transport problems, Vol. 6, No. 1, 2009, p. 43-48.
59. Afifi A., Ayzen S.: Statistical analysis. Mir, Moscow 1982.
60. Dynamic loads of freight car undercarriage. Ed. Kudryavtsev N.N. Tr. VNIIZHT. Issue 572, Transport, Moscow 1977.
61. Yessaulov V.P., Sładkowski A.W.: The use of MSC / NASTRAN for Windows for calculating of railroad wheels. [In:] Experience in the use of advanced computer technology for engineering analysis of MSC.Software Corporation in enterprises of Russia, Belarus, Ukraine. II Russian Conf. of MSC Users. Permanent mission of MSC.Software Corporation in CIS, Moscow 1999, p. 154-156.
62. Yessaulov V.P., Sładkowski A.W.: Determination of the finite element discretization error in the calculation of railway wheels. Problems of Strength, No. 5, 1990, p. 92-95.
63. Sitarz M., Sładkowski A. Definition of montage stresses in railway wheel pairs. [In:] Railway Wheel Set. Projecting. Producing. Operating. Repairing. Proc. of V Int. Sci. Conf. for Middle and Eastern European Countries, Silesian Technical University, Katowice 2002 (CD).